Protease-Activated Receptors in Embryonic Development

by

Courtney Timmons Griffin

DISSERTATION

Submitted in partial satisfaction of the requirements for the degree of

DOCTOR OF PHILOSOPHY

in

Biomedical Sciences

in the

GRADUATE DIVISION

of the

UNIVERSITY OF CALIFORNIA SAN FRANCISCO

Date University Librarian

Degree Conferred: .....

Dedication

Dedicated to my husband, Tim, whose faithful support makes me a stronger scientist.

Acknowledgements

I would like to acknowledge several people for their contribution to the work described in this dissertation. I inherited the *Par1-/-* embryonic lethality project from Andy Connolly, a former graduate student in the lab, who initially targeted PAR1 for deletion in mice and reported the finding of embryonic lethality at midgestation. Yoga Srinivasan, a post-doctoral fellow in the lab, made the TIE2p/e-PAR1 transgenic mouse used for rescue of the *Par1-/-* embryonic lethality phenotype and performed the initial experiments indicating that the transgene rescued lethality. Yoga also produced the *in situ* hybridization data in Chapter II showing specificity of the transgene for embryonic endothelium. Wei Huang maintained the embryonic stem cells and Yao Wu Zheng performed the blastocyst injection required for production of the PAR1-*LacZ* knock-in mouse described in Chapter IV. Additionally, Yao Wu Zheng made the constructs for the PAR4-*LacZ* and PAR2-*LacZ* knock-in mice described in Chapters III and IV. Throughout the course of these projects, I have been indebted to Rommel Advincula for his meticulous help in maintaining the various mouse colonies in our lab. I am also grateful for the numerous beautiful histological slides prepared by Linda Prentice that proved critical in interpreting the phenotype of *Par1-/-* embryos. Lastly, I have greatly benefited from my interaction with Shaun Coughlin and the many post-doctoral fellows, students, and technicians in his lab from 1995-2001.

PROTEASE-ACTIVATED RECEPTORS IN EMBRYONIC DEVELOPMENT

Courtney Griffin

Abstract

The blood coagulation cascade is best known as a sensor of vascular injury. The coagulation protease thrombin signals through protease-activated receptors (PARs) to achieve platelet aggregation, endothelial cell activation, and other important cellular responses to vascular leakage in the adult. However, coagulation factor knock-outs have also demonstrated an unexplained role for the cascade in the developing mouse embryo. Approximately half of PAR1-deficient embryos die at midgestation with massive hemorrhage due to defective vascular integrity. The receptor is expressed in embryonic endothelial cells, and we rescued death of *Par1-/-* embryos with an endothelial-specific PAR1 transgene. Our results highlighted a novel role for coagulation factor signaling in vascular development rather than in clot formation in the developing embryo. When PAR1 was targeted for deletion in combination with factor V, a cofactor necessary for thrombin production, virtually all doubly-deficient embryos died at midgestation, indicating the existence of other targets of coagulation proteases in embryonic development. We found that double-deficiency of PAR1 and PAR4, another thrombin receptor expressed in embryonic vasculature, resulted in 88% lethality. This result

suggests that PAR4 provides "back-up" signaling for PAR1 during embryonic development. The PARs are expressed throughout development, and *LacZ* knock-in technology allowed us to detect their expression in a number of novel tissues during late-gestation. This new information about the temporal and spatial expression of the PARs will potentially help us better understand the functional overlap and specificity of PAR signaling in both embryos and adults.

Table of Contents

List of Tables

List of Figures

Chapter I

INTRODUCTION

The blood coagulation cascade mediates biochemical responses to vascular injury [*1*]. Mechanical damage or inflammatory mediators cause leakage of plasma into extravascular spaces and subsequent activation of the cascade via contact between the extravascular membrane protein tissue factor and circulating protease zymogens. One of the key effectors of the cascade, the serine protease thrombin, is generated by cleavage of the coagulation zymogen prothrombin and performs two important functions in clot formation: fibrinogen cleavage and platelet activation. Fibrin monomers that polymerize to form the clot matrix are formed upon thrombin cleavage of the circulating glycoprotein fibrinogen. Platelet activation occurs as a result of a number of physiological effects caused by thrombin stimulation. Thrombin triggers platelet shape change and the release of platelet activators, chemokines, and growth factors. It also activates the integrin αIIb/β3 that binds fibrinogen and von Willebrand factor to mediate platelet aggregation [*2*]. In combination, these effects make thrombin the most potent stimulator of platelet aggregation known [*3,4*].

Thrombin stimulates a number of different cell types besides platelets to achieve cellular responses separable from clot formation. Most of these non-hemostatic roles have been determined through *in vitro* studies. For example, thrombin is a potent mitogen for a number of cells including cultured fibroblasts [*5*], smooth muscle cells [*6*], endothelium [*7*], and lymphocytes [*8*], perhaps implicating the protease in the stimulation of cell growth during *in vivo* wound-healing processes. Additionally, thrombin causes

chemotaxis in monocytes [*9*] and neutrophils [*10*] and cytokine/growth factor secretion from endothelial cells [*11*], smooth muscle cells [*12*], and lymphocytes [*8*], potentially as a means of stimulating inflammatory and/or immune responses to vascular injury. Other effects of thrombin on endothelium include shape change and induced permeability [*13*]—actions that may promote local extravasation of plasma proteins and edema at sites of vessel damage. Perhaps these proliferative, migratory, and permeability effects induced by thrombin on various cells *in vitro* can be unified by viewing thrombin as an orchestrator of tissue responses to vascular injury. Additionally, it is possible that these responses play a role in non-injury settings *in vivo*.

How does thrombin talk to cells? It does so through a small family of G protein-coupled seven transmembrane-spanning receptors called protease-activated receptors (PARs) [*1*]. The PARs are activated in a unique way: proteolytic cleavage (by thrombin or potentially other proteases) of their amino-terminal extracellular domain occurs at a specific site. This cleavage event unmasks a new amino terminus that then interacts with the body of the receptor to achieve intracellular signaling. Synthetic peptides designed to mimic the tethered ligands activate the receptors independently of cleavage [*14*]. PAR1, the first-discovered member of this family, was identified through an expression cloning strategy in Xenopus oocytes using mRNA from a human megakaryocyte-like cell line [*14*]. To date, two additional thrombin receptors—PAR3 and PAR4 [*15,16*]—have been identified. A potential trypsin [*17*] or tryptase [*18*] receptor, PAR2, which is also activated by coagulation factors VIIa and Xa [*19*], is the only other known PAR family member.

Only one thrombin receptor, PAR1, had been identified in 1994. In order to understand the *in vivo* implications of thrombin signaling in hemostasis/thrombosis, wound healing, and vascular disease, the receptor was targeted for deletion in mice [*20*]. The results were unexpected. *Par1-/-* mice showed no evidence of a bleeding diathesis; their platelets were activated normally in response to thrombin in platelet aggregation and secretion assays. The only defect originally associated with adult *Par1-/-* mice was an inability of their cultured lung fibroblasts to signal in response to thrombin [*20,21*]. This *in vitro* finding, however, had no effect on *in vivo* skin wound healing assays [*22*]. Because *Par1-/-* mice lacked a discernable phenotype, the evidence for the existence of another thrombin receptor was compelling. As a result, two more thrombin receptors—PAR3 and PAR4 [*15,16*]—were cloned. It is now understood that PAR1 is not a platelet thrombin receptor in the mouse. Instead, PAR3 and PAR4 are mouse platelet thrombin receptors. mPAR3 appears to function as a cofactor for mPAR4 cleavage and activation and does not confer signaling independently [*23*]. Therefore, targeted deletion of mPAR4 achieves the long-sought abolition of platelet activation by thrombin [*24*]. *Par4-/-* mice provide, at last, an opportunity to define the importance of thrombin-induced platelet activation in hemostasis and thrombosis.

One unexpected phenotype did emerge from the PAR1 knock-out that has served as the basis for this thesis. Approximately half of *Par1-/-* embryos die *en utero* at midgestation [*20,25*]. This finding has been recapitulated using different targeting strategies, targeted embryonic stem cell clones, and genetic backgrounds. A primary goal of this thesis is to elucidate and define the developmental roles of PAR1 and of other coagulation factors and effectors. In Chapter II we carefully describe the phenotype of

Par1-/- embryos. We find that *Par1-/-* embryos bleed to death due to defective vascular integrity. Significantly, *Par1-/-* embryos can be rescued by restoring receptor expression to endothelial cells. Our data provide strong evidence for *in vivo* thrombin signaling on endothelium during development. In Chapter III we use genetics to demonstrate that PAR1 is not the only effector of the coagulation cascade during development. A number of coagulation factors upstream of PAR1 had been knocked-out by other labs resulting in phenotypes grossly similar to our own—partial embryonic lethality at midgestation. We can increase lethality to almost 100% when we produce embryos doubly-deficient in coagulation factor V and PAR1. This chapter addresses the implications of our finding and provides evidence that PAR4 may provide redundant signaling with PAR1 during development. In Chapter IV we use *LacZ* knock-in technology to describe the expression patterns of PARs during embryonic development. PAR1-*LacZ* and PAR2-*LacZ* knock-in embryos, in particular, show us surprising sites of PAR expression and extend our current understanding of developmental protease signaling beyond midgestation.

Chapter II

A ROLE FOR THROMBIN RECEPTOR SIGNALING IN ENDOTHELIAL CELLS DURING BLOOD VESSEL DEVELOPMENT

ABSTRACT

Coagulation proteases mediate hemostatic and inflammatory responses to tissue injury [*2,26*]. We now report a role for cell signaling by a coagulation protease in a very different context--development of embryonic blood vessels. Protease-activated receptor-1 (PAR1) mediates cellular responses to the coagulation protease thrombin [*1*]. Approximately half of *Par1-/-* mouse embryos died at midgestation with bleeding from multiple sites and with defects in the walls of great vessels and in the yolk sac vasculature. PAR1 is highly expressed in embryonic endothelial cells [*27*] and, strikingly, a PAR1 transgene driven by the endothelial-specific *TIE2* promoter/enhancer elements prevented death of *Par1-/-* embryos. Our data show that PAR1 signaling in endothelial cells is important for vascular development. We suggest that PAR1 and the coagulation cascade may allow endothelial cells to sense and respond to the connectivity, permeability, density, or other properties of developing blood vessels.

RESULTS

Among their myriad roles, extracellular proteases can function like hormones to regulate cellular behaviors. Perhaps the best-studied example is that of thrombin, a multifunctional serine protease. Thrombin is the product of a highly regulated cascade of zymogen activation that is triggered when circulating coagulation factors meet tissue factor. Normally, tissue factor is expressed by cells that do not directly contact blood, but tissue factor can be expressed by cytokine-activated leukocytes and endothelial cells [*28,29*]. Thus, in the adult, thrombin generation occurs in the setting of tissue injury or inflammation. In this context, thrombin is best known for cleaving fibrinogen to fibrin monomer, which polymerizes to generate fibrin matrices important for hemostasis and response to infection [*2,30*]. Thrombin is also a potent activator of platelets, which are key effectors of hemostasis, and thrombin triggers a host of responses in endothelial cells, many of which can be viewed as proinflammatory [*1*]. These observations as well as the phenotypes associated with gain-of-function and partial loss-of-function mutations in coagulation factor genes in humans have cast the coagulation cascade and its effector protease thrombin in the role of orchestrating responses to tissue injury.

Cellular responses to thrombin are mediated, at least in part, by a family of protease-activated G protein-coupled receptors (PARs) for which PAR1 is the prototype [*1*]. Mouse embryos lacking PAR1 or coagulation factors die with varying frequency at midgestation, often with signs of bleeding [*20,31-37*]. The exact basis for embryonic death is unknown. We now report that PAR1 function in endothelial cells is important for hemostasis and vascular integrity during embryonic development. Our results suggest

that loss of thrombin signaling in endothelial cells rather than loss of platelet activation or fibrin formation likely accounts, in part, for the embryonic lethality caused by coagulation factor deficiencies. These findings highlight a role for the coagulation cascade and PARs in normal blood vessel development—a role beyond mediating responses to tissue injury.

Matings between *Par1*+/- and *Par1*-/- mice in a C57Bl/6J background (≥97%) yielded 135 *Par1*+/- and 73 *Par1*-/- progeny (*Par1*-/- =54% of expected; $p<<0.001$ by χ^2 test). Of the *Par1*-/- offspring, 36 were females, and 37 were males. These results confirmed the partial embryonic lethality initially reported in mixed 50%C57Bl/6J-50%129/Sv and in pure 129/Sv backgrounds [*20,25*]. The finding of similar frequencies of embryonic lethality in the C57Bl/6J and 129/Sv inbred backgrounds suggests that the partial penetrance of the *Par1*-/- phenotype is not due to the presence or absence of a modifier gene. Moreover, in a colony of *Par1*-/- mice maintained over five years, *Par1*-/- x *Par1*-/- matings continued to yield approximately 50% embryonic loss over ~15 generations with no evidence for a modifier gene.

Characterization of *Par1*-/- embryos was performed in the C57Bl/6J (≥97%) background and revealed hemorrhage at midgestation as the likely proximate cause of death. At E8.75, *Par1*-/- and wild-type embryos were indistinguishable by gross appearance and somite counts and were present in equal numbers in *Par1*+/- x *Par1*+/- litters (not shown). At E9.5, however, gross examination revealed blood in the exocoelomic and/or pericardial cavities in 22% of *Par1*-/- embryos. These embryos were pale, and their yolk sacs lacked blood-filled vessels. Embryos with gross bleeding

usually had a dilated pericardial sac, a sign of cardiovascular failure. By E10.5, bleeding was seen in 35% of *Par1-/-* embryos; pericardial bleeding was especially prominent (Fig. 1F). By E12.5, 52% of *Par1-/-* embryos were dead with evident bleeding. The remaining E12.5 *Par1-/-* embryos were alive and appeared normal.

Examination of histological sections revealed that bleeding occurred earlier and more frequently than was apparent by gross examination (Table 1). Extravascular blood cells were seen in sections of gravid uterine segments containing *Par1-/-* embryos as early as E9.0, before gross bleeding was detected. By E9.5, collections of blood cells were seen in the exocoelomic, amniotic, and/or pericardial and peritoneal cavities in 66% of *Par1-/-* embryos (Fig. 2). By contrast, no such collections were observed in 16 wild-type E9.5 embryos examined in parallel. Twelve of the 19 E9.5 *Par1-/-* embryos in which bleeding was evident by histology had not developed pericardial effusions or other apparent abnormalities, and, importantly, E9.5 and E10.5 embryos with both gross bleeding and vigorous heart beats were occasionally seen. By contrast, dead embryos always had evidence of bleeding. Thus, bleeding clearly precedes and probably causes the death of *Par1-/-* embryos at midgestation. The observation that most *Par1-/-* embryos show signs of bleeding by histology while only a fraction show gross bleeding raises the possibility that the extent of blood loss determines whether *Par1-/-* embryos die—a plausible explanation for the partial and apparently stochastic nature of embryonic loss.

Why do PAR1-deficient embryos bleed? Blood cells in the exocoelom of *Par1-/-* embryos were likely from the extraembryonic vasculature, while pericardial blood was

from the embryo proper. Such bleeding from multiple sites suggests a defect in hemostatic mechanisms or in the vasculature itself. It is difficult to attribute bleeding in *Par1-/-* embryos to defective platelet function because platelets from PAR1-deficient mice respond normally to thrombin [*20*] and because mice that lack platelets develop normally [*38*]. Furthermore, mature platelets have not been detected as early as E9.5 [*39,40*]. We therefore examined the possibility that bleeding in *Par1-/-* embryos might be due to a defect in the blood vessels themselves. RNA in situ hybridization suggests that PAR1 is highly expressed in endocardium and endothelium in E9.5 embryos [*27*]. To better characterize PAR1 expression, we generated PAR1-*LacZ* "knock-in" mice. β-galactosidase staining of E9.5 PAR1-*LacZ* knock-in embryos revealed PAR1 expression in endocardium and vascular endothelium, in occasional round cells adhering to the vessel wall, and in a subset of mesenchymal-appearing cells in the septum transversum, emphasizing the relatively restricted expression of PAR1 at E9.5 (see Chapter 4, Fig. 15). These results suggested that loss of PAR1 signaling in endothelial cells might underlie bleeding in *Par1-/-* embryos and prompted a search for morphological defects in the developing vasculature. Whole-mount PECAM staining and β-galactosidase staining of *Par1-/-* embryos carrying the endothelial-specific TIE2 promoter/enhancer-*LacZ* transgene (TIE2p/e-*LacZ*) [*41*] failed to reveal gross malformations of the embryonic vasculature. However, analysis of complete serial sections revealed a breach in the wall of the sinus venosus in two of three *Par1-/-* E9.5 embryos with gross pericardial bleeding (Fig. 2D). These openings appeared to be large enough to allow blood cells to enter the pericardial cavity from the vascular space and presumably account for the bleeding seen in these embryos. Similar defects were seen in other great vessels in serial sections of

uterine segments containing E9.5 *Par1-/-* embryos that were embedded *en bloc* before sectioning and are therefore unlikely to be artifacts of manipulation. In the extraembryonic vasculature, β-galactosidase staining of yolk sacs from E8.5 *Par1-/-* embryos carrying the TIE2p/e-*LacZ* transgene revealed a primary vascular plexus that was indistinguishable from wild-type. However, by E9.5, embryos with gross bleeding also showed abnormal β-galactosidase staining patterns—usually delayed vascular remodeling (Fig. 1, E and G). These vascular abnormalities in the embryo proper and yolk sac were noted only in embryos with gross bleeding, and it was possible that they were secondary phenomena. However, in the context of PAR1's expression pattern and the finding that bleeding preceded death, it seemed equally likely that these abnormalities were caused by a loss of PAR1 signaling in endothelial cells, which, in turn, caused bleeding and death.

The hypothesis that loss of PAR1 function in endothelial cells was the primary defect in *Par1-/-* embryos made a strong and testable prediction. Endothelial-specific expression of PAR1 should prevent death of *Par1-/-* embryos. We therefore generated transgenic mice in which the endothelial-specific *TIE2* promoter/enhancer elements (TIE2p/e) [*41*] drove mPAR1 expression. Two lines, one C57Bl/6J and one mixed DBA/2J-C67Bl/6J, were chosen for study. In each, in situ hybridization using the SV40 region of the transgene as a probe demonstrated selective expression of the transgene in endothelium and endocardium at midgestation (Fig. 3A). Endothelial-specific expression of the transgene in these mice was further supported by the observation that, unlike fibroblasts from wild-type mice, fibroblasts from *Par1-/-* mice bearing the transgene did not show thrombin-triggered increases in cytosolic calcium (Fig. 3B). We first crossed

Par1+/- mice hemizygous for the transgene (TIE2p/e-PAR1+/0:*Par1*+/-) with *Par1*-/- mice in the C57Bl/6J background. At E11.5-12.5, embryos were scored as alive or dead, then genotyped (Fig. 4A). Scoring was based on the presence or absence of a heartbeat, but by E11.5, embryos fell into two distinct groups—normal vs. grossly runted and/or necrotic. Strikingly, the death rate associated with PAR1 deficiency was 39% in transgene-negative embryos but only 14% in transgene-positive embryos ($p<<0.001$ by χ^2 test). The death rate for *Par1*+/- embryos was 6% independent of the transgene. Dead *Par1*-/- embryos lacking the transgene had pericardial effusions and bleeding, which were not seen among the dead transgenic null or *Par1*+/- embryos. In a second test of transgene rescue, we genotyped live offspring from crosses in the C57Bl/6J designed to yield equal numbers of transgenic and non-transgenic *Par1*-/- and *Par1*+/- mice (Fig. 4B). As before, *Par1*-/- offspring were generated at approximately half the expected frequency in the absence of the transgene, but transgene-positive *Par1*-/- pups were born at a frequency indistinguishable from heterozygotes. Similar results were obtained in an analogous study that used the DBA/2J-C67Bl/6J transgenic line (not shown). Thus, in three separate experiments, the TIE2p/e-PAR1 transgene greatly reduced or prevented death due to PAR1-deficiency in embryonic development. In both TIE2p/e-*LacZ* mice and TIE2p/e-PAR1 mice, transgene expression was detected only in endothelium and endocardium and in a small number of circulating cells (not shown). Taken together, our results strongly suggest that the death of *Par1*-/- embryos is due to a lack of PAR1 in endothelial cells.

DISCUSSION

Our results show that PAR1 function in endothelial cells contributes to hemostasis and vascular integrity in the developing mouse embryo. It is likely that loss of PAR1 signaling in endothelial cells explains, at least in part, impaired hemostasis and death at midgestation caused by knockout of tissue factor [*31-33*], factor V [*35*], and prothrombin [*36,37*]. What is it that the coagulation cascade and PARs sense during development, and which endothelial cell responses to PAR1 activation might be important for hemostasis and vascular integrity during development? In the adult, PARs provide a mechanism for cells to sense activation of the coagulation cascade, which occurs when plasma coagulation factors access the extravascular space. Thus, in the embryo it is possible that PAR1 and the coagulation cascade allow developing blood vessels to monitor their integrity and to mount an acute hemostatic response to occasional breaks that spontaneously arise. Thrombin triggers mobilization of P-selectin and von Willebrand factor to the endothelial cell surface [*42*]. In the adult, this response may contribute to hemostasis by recruiting leukocytes and platelets to sites of endothelial activation and by indirectly promoting thrombin generation and fibrin deposition [*43,44*]. However, neither platelets nor fibrinogen appear to be important for hemostasis at E9.5 [*24,38-40,45,46*]. It is possible that endothelial activation by thrombin mediates acute hemostatic responses in the embryo by a novel mechanism. Perhaps, however, PAR1 signaling in endothelial cells plays a role in proper development of the blood vessels themselves. For example, the coagulation cascade and PARs may provide a means for leaky nascent vessels to sense their permeability to plasma proteins in an ongoing way

and to modify their structure accordingly. Or they may allow blood vessels to simply check that they are properly connected to the circulation (that is, to a source of plasma coagulation factors). In addition, this system might provide a means of sensing hypoxia, which can both increase endothelial permeability and induce tissue factor expression in a variety of cell types [*47-49*]. This raises the additional possibility that the coagulation cascade and PARs might provide one means for the developing vasculature to sense inadequate tissue perfusion and to grow and remodel in appropriate ways. Thrombin causes endothelial cells to change shape, increases the permeability of endothelial cell monolayers [*50*], disrupts VE-cadherin complexes and cell-cell junctions [*51*], and promotes endothelial cell proliferation [*7*]. Thrombin also stimulates endothelial cells to secrete extracellular matrix proteins [*52*] and growth factors such as PDGF [*11*] and enhances responsiveness to the endothelial cell mitogens VEGF [*53*] and FGF [*7*]. Thus PAR1 activation might contribute to vascular development by regulating endothelial cell shape, movement, proliferation, and/or interactions with nearby cells and extracellular matrix. Overall, our results highlight a new role for the coagulation system: directly regulating endothelial cell function during blood vessel formation in embryonic development.

METHODS

Breeding. *Par1-/-* [*20*] mice that had been backcrossed into the C57Bl/6J background (>97%) were used. TIE2p/e-*LacZ* [*41*] transgenic mice (kindly provided by Tom Sato) were bred with *Par1-/-* mice. To generate precisely timed pregnancies, matings were restricted to a 1 hour interval (8 a.m.-9 a.m.) with 9 a.m. counted as E0. In other cases, matings were set up overnight, and females were checked for vaginal plugs each morning before 10 a.m. Noon on the day of plug detection was counted as E0.5.

Genotyping. Genotypes were assessed by Southern blot analysis of genomic DNA from embryonic or yolk sac tissue. For PAR1, genomic DNA was digested with *XbaI* and probed with a 308 bp fragment of intron sequence immediately 3' of PAR1 exon 2 (generated by PCR with forward primer 5'-ATTTACTACTACGCCTCCTCCGAG and with reverse primer 5'-AGCAGAAGTATTCGTGCATATCGG). This identified 0.7 and 2.2 kb bands for the targeted and wild-type alleles, respectively. For the TIE2p/e-PAR1 transgene, the PAR1 probe was used and detected the transgene as a 7 kb *XbaI* fragment.

TIE2p/e-PAR1 Transgenic Construct. A 1.2 kb *EcoRI/XbaI* (blunted) fragment containing the mPAR1 cDNA coding region was inserted 5' to an 847 bp fragment of SV40 small t intron and polyA sequence from the vector CPV2 [*54*] in pBluescript SK (Stratagene). A 2.1 kb *HindIII* fragment containing the TIE2 promoter and a 9 kb fragment containing the TIE2 enhancer from pHHNS [*41*] (kindly provided by Tom Sato) were inserted 5' and 3' to the 2 kb PAR1-SV40, respectively. The resulting 13.1 kb insert was used for microinjections.

Histology. To analyze embryos for microscopic bleeding, pregnant mice were euthanized and perfusion-fixed with 4% PFA. Whole gravid uterine segments were then removed *en bloc* to avoid artifacts related to dissection, immersion-fixed overnight, dehydrated, embedded in paraffin, sectioned (10μm), and stained with hematoxylin and eosin.

β-galactosidase Staining, Immunohistochemistry, and In Situ Hybridization. Whole mount β-galactosidase staining and immunostaining for PECAM [*55*] and in situ hybridization for PAR1 mRNA [*27*] were performed as described. In situ hybridization for TIE2p/e-PAR1 transgene mRNA was performed using probe transcribed from the 847 bp SV40 small t intron and polyA fragment included in the transgene [*54*].

dpc	Gross bleeding	Microscopic bleeding
E8.75	0/24 (0%)	0/7 (0%)
E9.0	0/6 (0%)	2/15 (13%)
E9.5	18/83 (22%)	19/29 (66%)
E10.5	11/31 (35%)	----------
E12.5	12/23 (52%)	----------

Table 1: Numbers of *Par1-/-* embryos with bleeding at various stages. *Par1-/-* embryos were assessed for bleeding at various gestational ages (dpc=days post coitum). Gross bleeding was defined as visible blood pooled in the pericardial or exocoelomic cavities of dissected embryos. Microscopic bleeding was assessed in sections of gravid uterine segments embedded *en bloc* (i.e., minimally manipulated) and was defined as collections of embryonic blood cells in the pericardial/peritoneal, amniotic, and/or exocoelomic cavities (see Fig. 2).

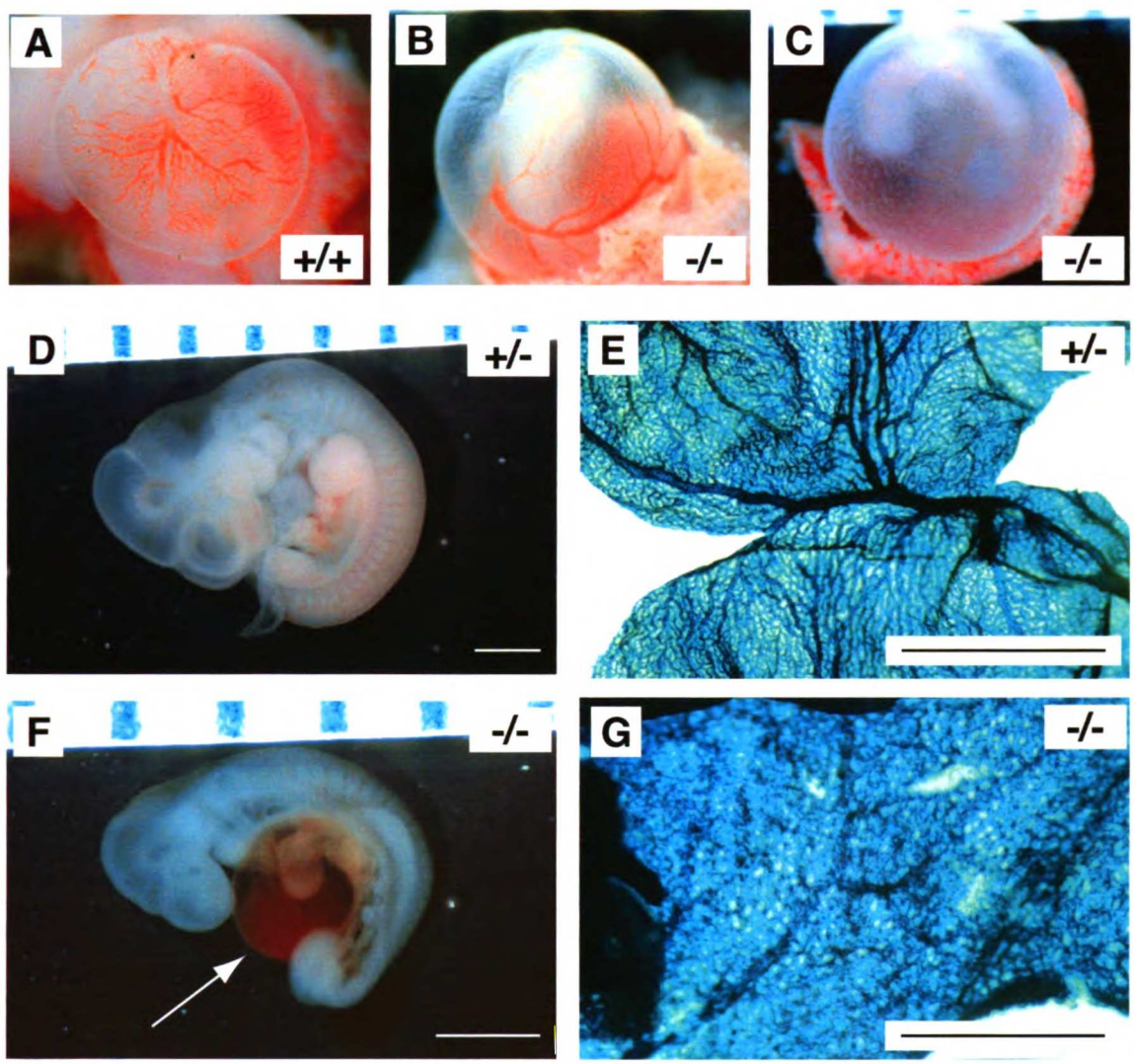

Fig. 1: Gross phenotype of *Par1-/-* embryos at midgestation.
A-C: E9.5 embryos surrounded by their undissected yolk sacs. Wildtype (**A**) and 78% of *Par1-/-* yolk sacs (**B**) are complexly vascularized with vessels containing visible embryonic blood by E9.5. 22% of *Par1-/-* embryos, however, are dead at E9.5 and are surrounded by yolk sacs lacking visible embryonic blood (**C**). **D**,**F**: *Par1+/-* (**D**) and *Par1-/-* (**F**) littermate E10.5 embryos. Note the dilated, blood-filled pericardial cavity (arrow) in the *Par1-/-* embryo. **E**,**G**: Yolk sacs from the embryos shown in (**D**) and (**F**), respectively. These embryos carried a TIE2p/e-*LacZ* transgene to allow visualization of the vascular endothelium. β-galactosidase-stained yolks sacs are shown. Scale bars: 1mm.

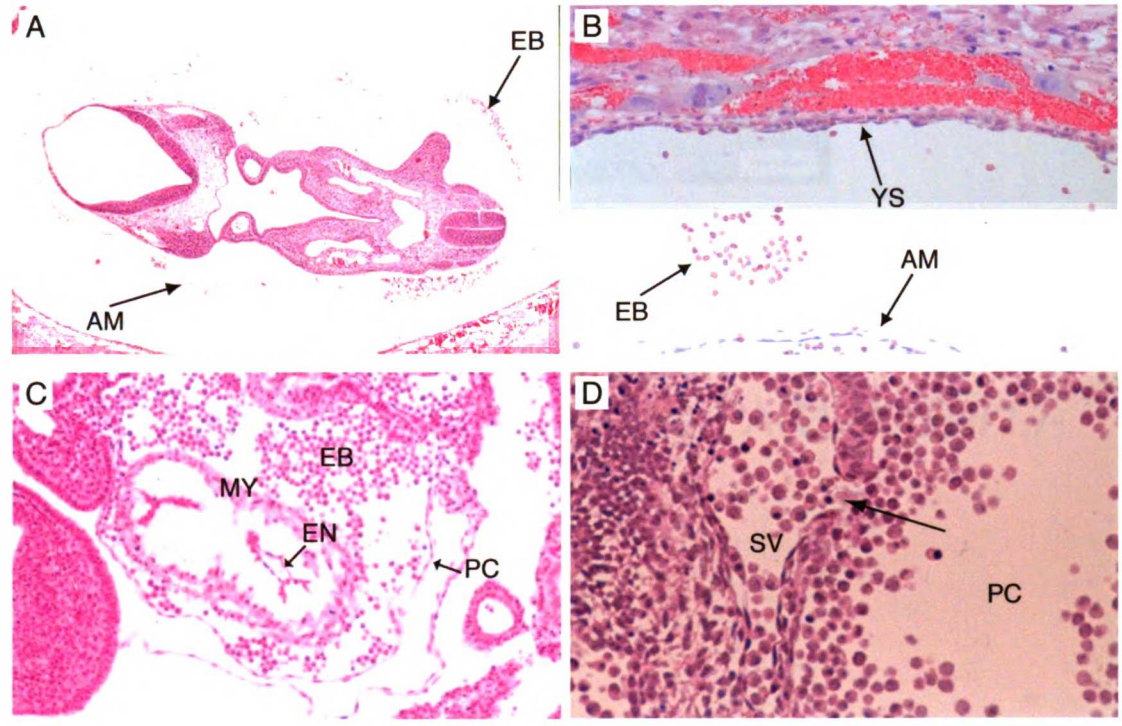

Fig. 2: Bleeding and vascular defects of *Par1-/-* embryos.
A: An *en utero* section from an E9.5 *Par1-/-* embryo is shown with pooled embryonic blood (EB) in the amniotic cavity (AM) (4x). **B**: An *en utero* section from an E9.5 *Par1-/-* embryo is shown with pooled embryonic blood (EB) in the exocoelomic cavity between the yolk sac (YS) and the amnion (AM) (20x). **C**: Section from a *Par1-/-* embryo with gross pericardial bleeding is shown. Extravascular embryonic blood (EB) is shown in the pericardial cavity (PC). The myocardium (MY) and endocardium (EN) of the ventricle are indicated (10x). **D**: Section from an E9.5 *Par1-/-* embryo with gross pericardial bleeding reveals a defect (arrow) in the wall of the sinus venosus (SV) large enough to allow entry of blood cells into the pericardial cavity (PC) (30x).

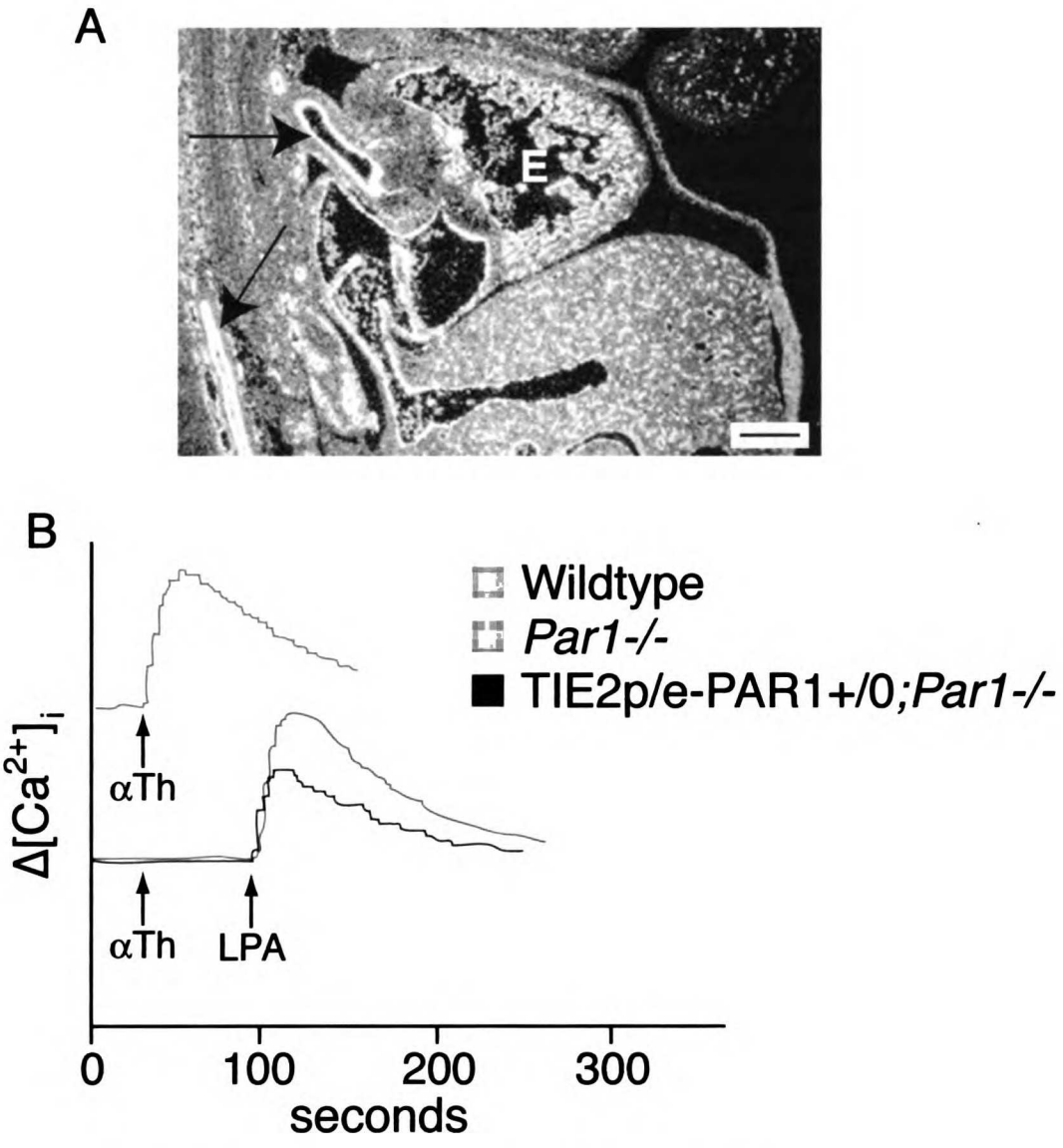

Fig. 3: Endothelial specificity of the TIE2p/e-PAR1 transgene. **A:** *In situ* hybridization for the SV40 sequence tag mRNA of an E13.5 embryo hemizygous for the TIE2p/e-PAR1 transgene. Note silver grains indicating expression of the transgene overlying endocardium (E) and endothelium of the great vessels (arrows) and microvasculature. Similar results were obtained with an E9.5 embryo. Scale bar: 250μm. **B**: Cytosolic calcium transients in wildtype, *Par1-/-*, and TIE2p/e-PAR1+/0;*Par1-/-* fibroblasts. Increases in intracellular calcium in response to thrombin (aTh; 30nM) or lysophosphatidic acid (LPA; 5μM) were determined using Fura-2. Agonists were added at the indicated times. Note lack of response to thrombin in the TIE2p/e-PAR1+/0;*Par1-/-* fibroblasts.

A

	Par1+/-	*Par1-/-*
Tg+/0	6% (3/48)	14% (5/37)
Tg0/0	6% (2/33)	39% (11/28)

% DEAD (dead/total embryos)

B

	Par1+/-	*Par1-/-*
Tg+/0	52	51
Tg0/0	54	24

LIVE OFFSPRING

Fig. 4: Endothelial expression of PAR1 rescues *Par1-/-* lethality.
A: *Par1-/-* females were mated with TIE2p/e-PAR1+/0:*Par1+/-* males; the resulting E11.5-12.5 embryos were scored as dead or alive based on the absence or presence of a heartbeat, then genotyped by Southern analysis. Note decreased death of transgene-positive *Par1-/-* embryos.
B: Matings between TIE2p/e-PAR1+/0:*Par1-/-* x *Par1+/-* mice and TIE2p/e-PAR1+/0:*Par1+/-* x *Par1-/-* mice were performed, and offspring were genotyped at weaning. Note rescue of *Par1-/-* mice by transgene.

Chapter III

PAR1 IS NOT THE ONLY EFFECTOR OF THE COAGULATION CASCADE DURING DEVELOPMENT

ABSTRACT

Targeted deletion of the thrombin receptor PAR1 results in 50% embryonic lethality at midgestation [*20*]. Deficiency of factor V (FV), a cofactor necessary for thrombin production, results in a similar phenotype [*35*]. We found that in combination, 96% of embryos deficient in both FV and PAR1 died at midgestation suggesting that the genes function in intersecting pathways—rather than in a linear one. Since our data indicated that thrombin might have additional functions in development besides activating PAR1, we sought proteins downstream of factor V that would respond to thrombin during development and would increase lethality of PAR1-deficient embryos. We found that fibrinogen, a target of thrombin cleavage during adult hemostasis, did not increase lethality of *Par1-/-* embryos when knocked out. However, double-deficiency of PAR1 and PAR4, another thrombin receptor with a similar expression pattern to PAR1 but without any embryonic lethality of its own when targeted for deletion [*16,24*], resulted in 88% lethality. Our results indicate that PAR4 and PAR1 signaling pathways are largely redundant at midgestation and that the combined loss of PAR1 and PAR4 signaling likely accounts for the 85-100% lethality observed in tissue factor-deficient [*31-33*] and *Par1-/- FV-/-* embryos.

RESULTS

Is thrombin the endogenous activator of endothelial PAR1 during embryonic development or might PAR1 mediate responses to other proteases or even peptide agonists in this setting? Deficiencies of a number of coagulation factors upstream of PAR1, including prothrombin and factor V, a cofactor necessary for thrombin production, cause varying degrees of partial embryonic lethality at midgestation (Fig. 5) [*31-37*]. Perhaps these findings are to be expected since human patients with complete deficiency of prothrombin [*56*], FV [*57-59*], or FX [*60*] are rarely encountered, and human tissue factor deficiency has never been described, indicating that thrombin generation may be a critical requirement for human embryogenesis as well as for the mouse. In the mouse, approximately half of factor V-deficient (*FV-/-*) embryos die between E9.5-10.5 with multiple abnormalities, including hemorrhage [*35*], and approximately half of prothrombin-deficient embryos die between E9.5-11.5. Bleeding is described in one report [*36*] but not in another [*37*]. Thus, *Par1-/-*, *FV-/-*, and *Prothrombin-/-* embryos die at similar rates and times and perhaps from the same cause—bleeding. These observations suggested a simple linear pathway in which factor V and prothrombin triggered thrombin signaling via PAR1 during development (Fig. 6). If this pathway were accurate, the phenotype resulting from combined deficiency of PAR1 and factor V should have been identical to that of either deficiency alone. This was not the case. Indeed, a comparison of the phenotypes of embryos deficient in PAR1 or factor V to those lacking both genes revealed synthetic lethality (Fig. 7). The 4% survival rate of *FV-/-Par1-/-* embryos was markedly less than that of either *Par1-/-* or *FV-/-* embryos

(52% or 67% at E12.5, respectively, in this experiment) and significantly less than the 35% survival rate predicted if PAR1 and factor V deficiencies had caused death independently. The 22 dead *FV-/-Par1-/-* embryos were pale, runted, and severely necrotic with pericardial effusions and blood pooled in their pericardial and exocoelomic cavities. The nearly complete lethality and the phenotype of *FV-/-Par1-/-* embryos was similar to that reported for embryos deficient in tissue factor [*31*], the trigger for coagulation. These results suggest that the factor V and PAR1 pathways interact, refute the simple model in Fig. 6, and raise intriguing new possibilities (Fig. 8). The observation that PAR1 deficiency enhanced death of *FV-/-* embryos implies that PAR1 can be activated in the absence of embryonic factor V and raises the possibility that molecules other than factor V and thrombin can mediate activation of prothrombin and PAR1, respectively, during development (Fig 8). We cannot prove this conclusion rigorously because maternal factor V from the *FV+/-* mothers (used by necessity in these experiments [*35*]) might enter the embryonic circulation and support some thrombin signaling via PAR1; loss of such signaling might then account for the effect of PAR1 deficiency in *FV-/-* embryos. By contrast, the observation that factor V deficiency enhanced death of *PAR1-/-* embryos clearly implies that factor V has actions beyond activating PAR1 during development (Fig. 8). Thus, taken together, our observations suggest that thrombin and/or another factor V-dependent agonist act on PAR1 and on other targets and that these targets function in interacting pathways during embryonic development.

One obvious candidate for an additional thrombin substrate in a potentially interacting pathway was fibrinogen, which, although not necessary for development in

otherwise normal embryos [*46*], might become important in the context of the bleeding seen in PAR1-deficient embryos. However, in contrast to factor V deficiency, fibrinogen deficiency did not enhance death of *Par1-/-* embryos at E12.5 (Fig. 9). It is possible that fibrinogen from the *Fib+/-* mothers (used by necessity in these studies [*46*]) might have entered the embryonic circulation in sufficient quantity to prevent an embryonic phenotype, but, at face value, this negative result suggests that still other coagulation protease substrates are important for embryonic development. Platelets are not good candidate substrates since mature platelets have not been detected as early as E9.5—the time when FV-deficient and PAR1-deficient embryos die [*39,40*]. It is certainly possible, however, that other PARs are substrates for thrombin during development. RNAse protection assays demonstrate that *Par3* and *Par4* mRNAs are expressed in embryonic and extraembryonic tissue at E9.5 (Fig. 10). The notion that other PARs might in part compensate for PAR1 deficiency offers one explanation for the partiality of the PAR1 phenotype and is testable using mice with multiple PAR deficiencies.

We chose to analyze the lethality of *Par1-/-Par4-/-* embryos. PAR1 and PAR4 play redundant roles on human platelets but respond to different concentrations of thrombin [*1,61,62*]. We analyzed PAR4 expression in E9.5 embryos to determine whether the receptor was expressed in a pattern similar to that of PAR1 at midgestation (Fig. 11). β-galactosidase staining of homozygous PAR4-*LacZ*(neo-) embryos proved that PAR4 was, in fact, expressed in a vascular pattern reminiscent of PAR1's expression pattern at E9.5 (see Chapter 4, Fig. 15 for PAR1 expression). This was the first evidence of vascular PAR4 expression during development; β-galactosidase staining of PAR4-*LacZ*(neo-) embryos was initially carried out at later stages of development and only

revealed staining in the liver and gut (unpublished observations of Yao-Wu Zheng). The overlapping vascular expression of PAR1 and PAR4 increased our interest in a possible redundant signaling role for the receptors at midgestation. Individually, *Par4-/-* mice survive development without any detectable lethality [*24*]. In order to determine whether PAR4-deficiency could exacerbate *Par1-/-* embryonic lethality, we performed two types of matings: *Par1-/-Par4+/-* males and females were mated, and *Par4-/-Par1+/-* males and females were mated (Fig. 12). Only 12% of the doubly-deficient mice expected from matings between *Par4-/-Par1+/-* parents were born ($0.001>>p$ by χ^2 analysis of rates expected from a Mendelian distribution) (Fig. 12A). The 88% lethality of *Par1-/-Par4-/-* embryos was also significantly different than the expected lethality rate of 50%, which accounted for previously characterized *Par1-/-* lethality ($0.01>p>0.005$ by χ^2 analysis). 35% of doubly-deficient mice expected from matings between *Par1-/-Par4+/-* parents survived birth ($0.025>p>0.01$ by χ^2 analysis of rates expected from a Mendelian distribution) (Fig. 12B). The average litter size from these matings was 68% of the average litter size from matings between *Par4-/-Par1+/-* parents, presumably due to the 50% embryonic lethality observed in *Par1-/-* embryos. Therefore, the combination of 65% observed lethality and the presumed 50% unseen embryonic lethality brought the total lethality of doubly-deficient embryos from *Par1-/-Par4+/-* matings to 82% ($0.001>>p$ by χ^2 analysis against 50% overall *Par1-/-* lethality). Our results indicated that a combined loss of PAR1 and PAR4 signaling (due to loss of thrombin production) appeared to account for the 85-100% lethality observed in tissue factor-deficient and *Par1-/-FV-/-* embryos and that PAR4 is another developmental effector of the coagulation cascade.

DISCUSSION

The nearly complete lethality observed in our *Par1-/-FV-/-* embryos is reminiscent of the lethality observed in tissue factor (TF)-deficient mice [*31-33*]. Tissue factor is this only coagulation factor that when targeted for deletion in the mouse resulted in almost 100% embryonic lethality. In the hands of two groups, 0-1.3% of *TF-/-* embryos survived until birth [*31,32*]. Another group found perinatal survival rates of 14% in a mixed C57Bl/6-129/Sv background versus 0% in a Sv/129 background [*63*]. *TF-/-* lethality is speculated to be more penetrant than the 30-50% lethality seen in *FX-/-*, *FV-/-*, and *Prothrombin-/-* embryos due to the fact that tissue factor is membrane bound. The circulating maternal coagulation factors are thought to be capable of leaking through the yolk sac and placenta to supply "null" embryos with enough cascade activity for partial rescue. For example, deficiency of factor VII (FVII), the only known tissue factor ligand, was not found to cause death at midgestation, presumably due to the transplacental passage of exogenous factor VII that achieved embryonic levels of 0.06% of maternal levels by E11.5 [*39*]. Unfortunately, clean experiments in coagulation factor-deficient mothers cannot be performed because *FVII-/-*, *FX-/-*, *FV-/-*, and *Prothrombin-/-* embryos that survive midgestation die perinatally due to massive hemorrhage. However, the data generated from our cross between FV-deficient and PAR1-deficient mice were consistent with the hypothesis that maternal coagulation factors could support some level of thrombin activation and embryonic rescue.

The increased lethality in *Par1-/-Par4-/-* embryos supported the hypothesis that other PARs, in addition to PAR1, could be targets of developmental thrombin signaling.

However, the 88% lethality seen in our *Par1-/-Par4-/-* embryos was not as penetrant as the 100% lethality reported in *TF-/-* embryos [*31*]. While it is most likely that this penetrance discrepancy is due to differences in background strains (*TF-/-* lethality was as low as 86% in one report [*63*]), it is still possible that another PAR could provide redundant signaling with PARs1 and 4. In the adult, mPAR3 does not mediate transmembrane signaling itself but instead functions as a cofactor for PAR4 cleavage and activation at low concentrations of thrombin [*23*]. Nothing is known, however, of PAR3's signaling capabilities during development, although PAR3-deficient embryos survive development without apparent lethality. By *in situ* hybridization, PAR3 mRNA is expressed in liver and gut at E13.5, which is a similar expression pattern to that of PAR4 as detected by β-galactosidase staining of PAR4-*LacZ*(neo-) embryos at this time (unpublished observations of Yoga Srinivasan and Yao Wu Zheng, respectively). Perhaps the overlapping expression patterns of PAR3 and PAR4 at E14.5 are indicative of their co-factoring roles in development. Furthermore, *Par3* and *Par4* mRNAs are expressed in similar ratios in embryonic versus yolk sac tissue by RNAse protection at E9.5 (Fig. 10), providing further evidence of potential developmental co-factoring roles for the receptors. However, it's possible that PAR3 has an independent signaling role at midgestation; embryos deficient in PAR1, PAR3, and PAR4 would address this possibility. PAR2 is not thrombin receptor, but it has been shown to be activated by FVIIa/FXa in the presence of tissue factor [*19*]. PAR2-deficiency imparts no embryonic lethality in a mixed genetic background but imparts partial lethality in late-gestation embryos in a C57Bl/6J background (unpublished observation of Gilbert Sambrano). Its role in mouse embryos and adults is not understood, although it is postulated to be a

trypsin receptor. Our lab has hypothesized that PAR2 could play a role in coagulation cascade signaling (to FVIIa/FXa) that is redundant to that of PAR1 at E9.5. However, the expression pattern of PAR2 mRNA at midgestation does not support this hypothesis. β-galactosidase staining of PAR2-*LacZ*(neo-) knock-in embryos at E8.5 and E9.5 shows the receptor restricted to the cells lining the neural ridge (see Chapter 4, Fig. 21). This pattern is vastly different from that of PAR1 and PAR4 expression at E9.5, which is primarily vascular. Therefore, unless PAR2 is expressed in endothelium at levels too low to be detected by β-galactosidase staining, it is unlikely that the receptor performs a redundant signaling role with PAR1 and PAR4 during development. Finally, our observation of incomplete lethality of *Par1-/-Par4-/-* embryos versus 100% lethality reported in *TF-/-* embryos suggests that an unknown thrombin (or FVa) receptor could exist during development. A search for an embryonic receptor might be performed using an expression cloning approach in *Xenopus* oocytes analogous to that used to clone PAR1 [*14*]. Ultimately, a careful study of E12.5 *Par1-/-Par4-/-* embryos, analogous to that performed on *Par1-/-FV-/-* embryos, will provide a better understanding of the true lethality rate and phenotype of *Par1-/-Par4-/-* embryos. Such a study will help better determine whether additional thrombin signaling—beyond that mediated by PAR1 and PAR4—could be occurring at midgestation.

METHODS

Breeding. *FV+/-* [*35*], *Fib+/-* [*46*] (generous gifts from David Ginsburg and Jay Degen, respectively) and *Par1-/-* [*20*] mice that had been backcrossed into the C57Bl/6J background (>97%) were used. *Par4-/-*[*24*] mice from a mixed background (50%C57Bl/6J-50%129/Sv) were used. Matings were set up overnight, and females were checked for vaginal plugs each morning before 10 a.m. Noon on the day of plug detection was counted as E0.5.

Genotyping. Genotypes were assessed by Southern blot analysis of genomic DNA from embryonic or yolk sac tissue. For PAR1, genomic DNA was digested with *XbaI* and probed with a 308 bp fragment of intron sequence immediately 3' of PAR1 exon 2 (generated by PCR with forward primer 5'-ATTTACTACTACGCCTCCTCCGAG and with reverse primer 5'-AGCAGAAGTATTCGTGCATATCGG). This probe identified 0.7 and 2.2 kb bands for the targeted and wild-type alleles, respectively. For factor V, genomic DNA was digested with *HpaI* and probed with a 2.2 kb *NdeI-PstI* fragment of FV exon 13 yielding 9.2 and 14.4 kb bands for the targeted and wild-type alleles, respectively. Fibrinogen was genotyped using a *PvuII* genomic digest and "Probe A" as described [*46*]. For PAR4, genomic DNA was digested with HindIII and probed with a 470 bp fragment of sequence spanning 140 bp of the 3' end of mPAR4 exon 2 plus 330 bp of the 3' untranslated region (generated by PCR with forward primer 5'-CCCATGAGTTCAGGGAGAAGGT and with reverse primer 5'-AGAAACCAGAATGGAGTTTCCC). This probe identified 9 kb and 2.5 kb bands for the targeted and wild-type alleles, respectively.

RNAse Protection Assay (RPA). RPAs were performed using the RPAII kit from Ambion (catalog #1410). Total RNAs from adult mouse tissues were obtained by mechanical homogenization of organs and subsequent purification with TRIzol Reagent (Gibco, catalog #15596-026). Total RNAs from pooled littermate embryos (with matching somite numbers) or their yolk sacs were also obtained by mechanical homogenization and subsequent purification with TRIzol Reagent. Total RNAs were quantified by spectrophotometric analysis.

β-galactosidase staining. PAR4-*LacZ* knock-in embryos [*24*] were dissected free of maternal tissue and were fixed in 2% paraformaldehyde/0.2% glutaraldehyde. Embryos were rinsed in PBS and stained in the dark for 72 hours at room temperature in X-gal solution (5μM Potassium Ferricyanide, 5μM Potassium Ferrocyanide, 2μM $MgCl_2$, 1mg/ml X-gal in PBS). Blue embryos were washed in PBS and post-fixed in 4% paraformaldehyde.

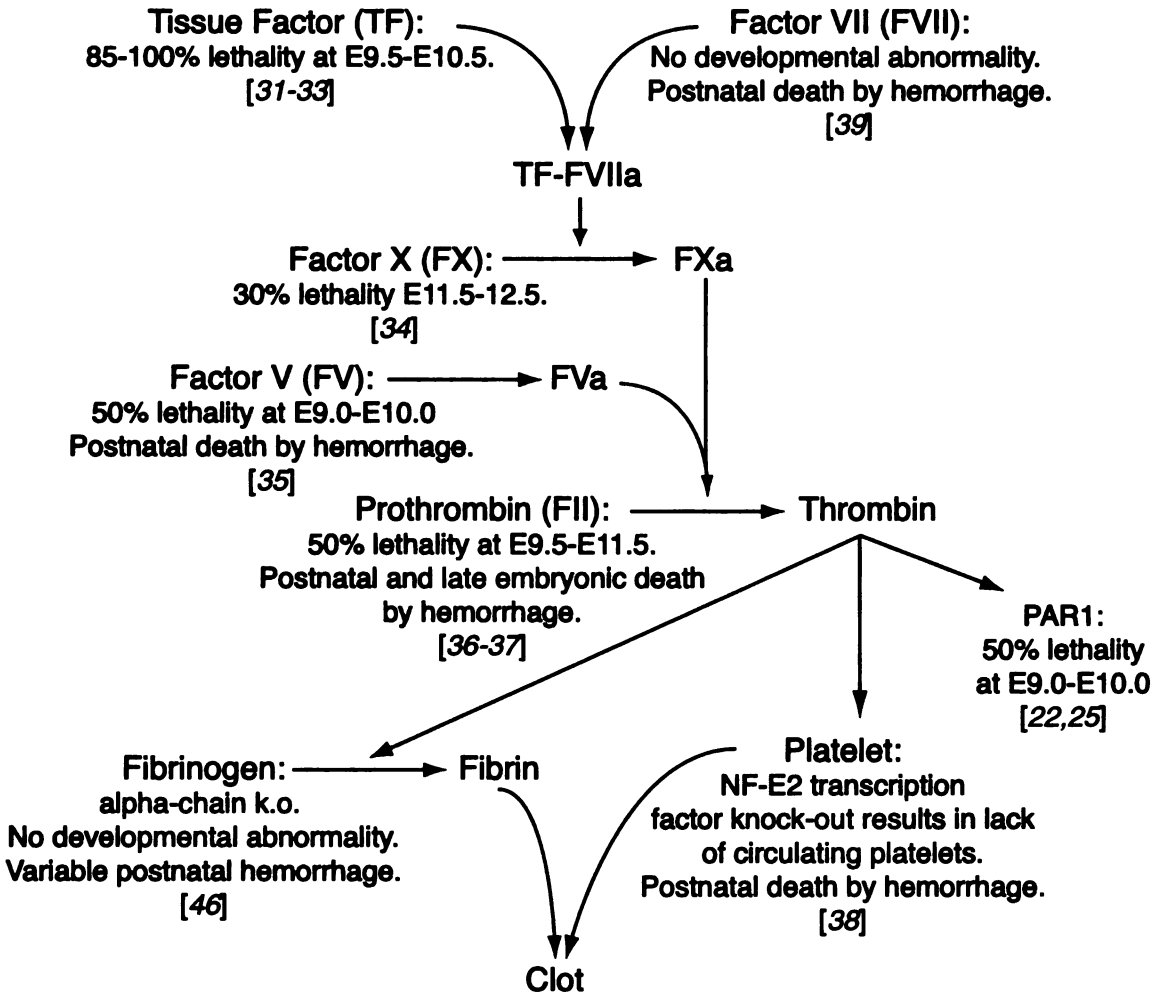

Fig. 5: Published coagulation factor knock-out phenotypes.

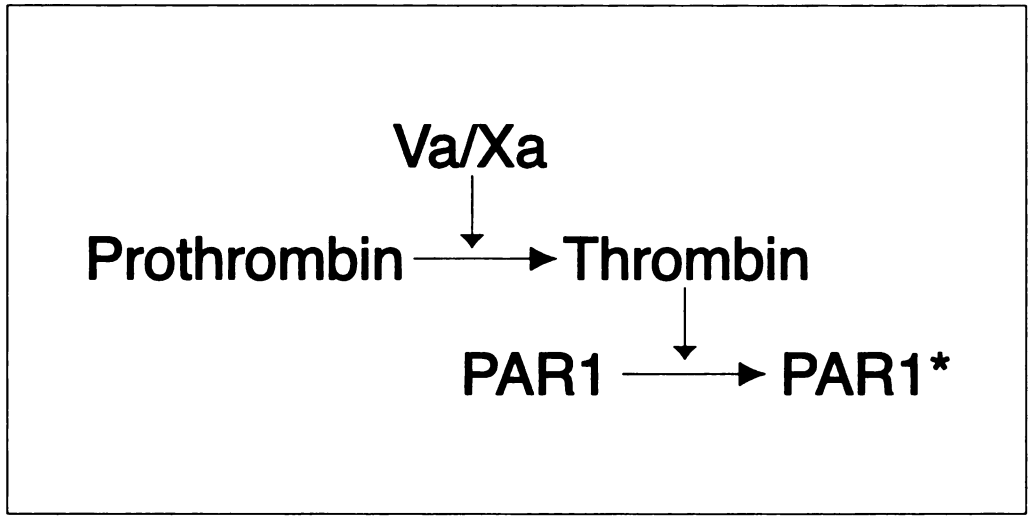

Fig. 6: Role of factor V and PAR1 in development: initial model. A simple linear pathway in which activated factors V and X (Va/Xa) trigger conversion of prothrombin to thrombin that then activates PAR1.

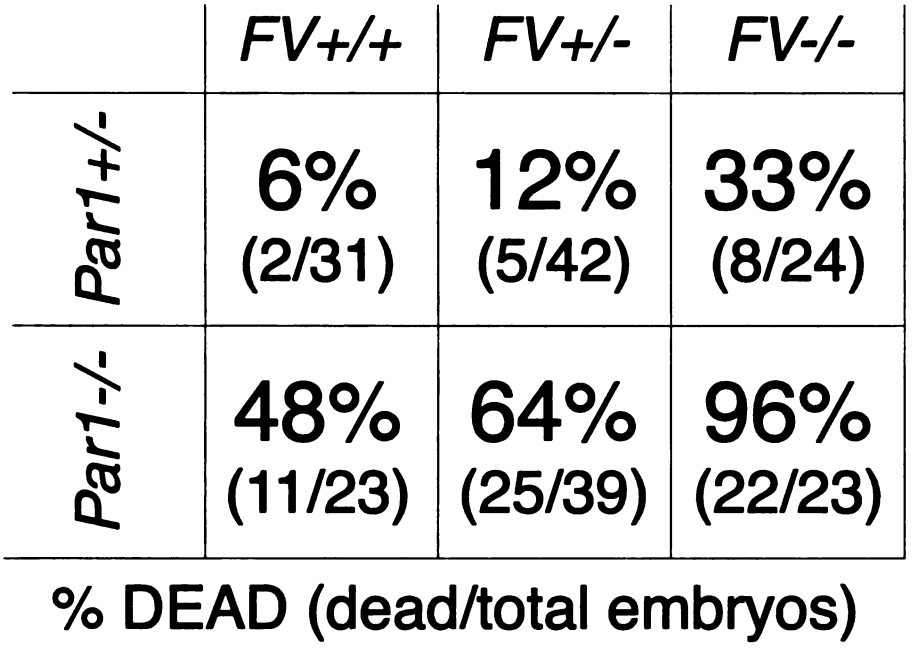

Fig. 7: Factor V-deficiency augments *Par1-/-* embryonic lethality. *FV+/-Par1+/-* females were mated with *FV+/-Par1-/-* males. E11.5-12.5 embryos were scored dead or alive and genotyped by Southern analysis. Note virtually complete lethality for doubly-deficient embryos ($p<0.001$ by $\chi 2$ test vs. any other group).

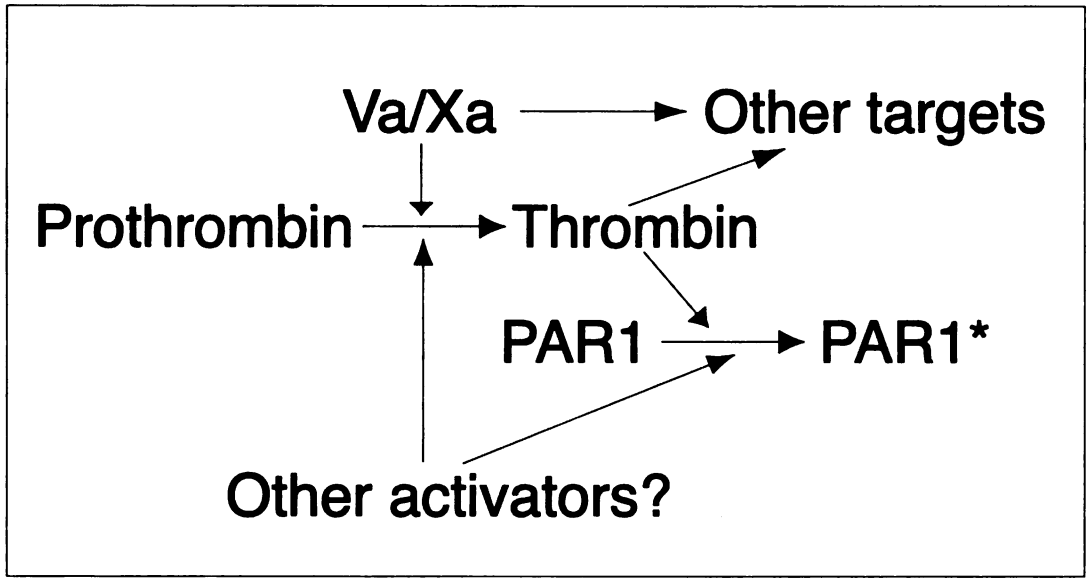

Fig. 8: Role of factor V and PAR1 in development: revised model. Note PAR1-independent actions of factor V and possible alternative routes to PAR1 activation to account for the data shown in Figure 6.

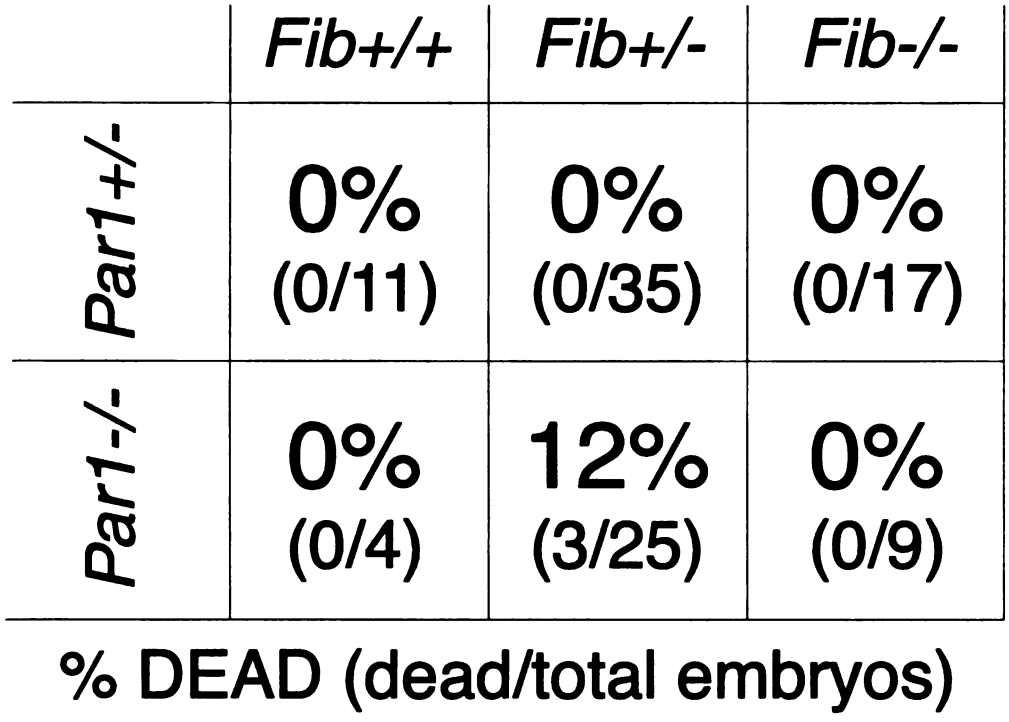

Fig. 9: Fibrinogen-deficiency does not augment *Par1-/-* embryonic lethality. *Par1-/-Fib+/-* males were mated to *Par1+/-Fib+/-* females. E11.5-12.5 embryos were scored dead or alive and genotyped by Southern analysis. In addition to the 101 embryos genotyped, 8 dead embryos were ungenotypable due to lack of tissue.

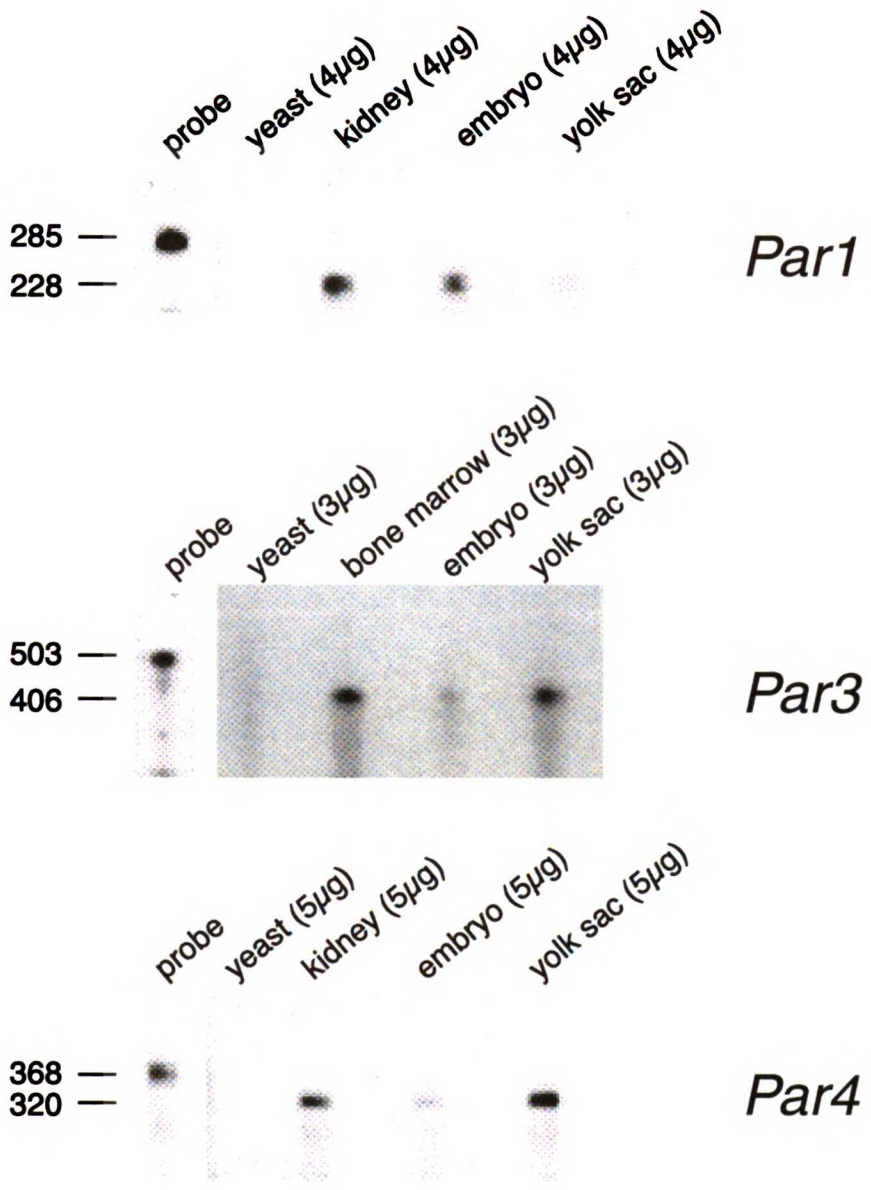

Fig. 10: Relative expression levels of PAR mRNAs at E9.5.
Total RNA was obtained from wildtype E9.5 embryos and yolk sacs and was analyzed by RNAse Protection Assay for expression of PAR mRNAs. Yeast tRNA and total RNA from selected adult organs were used as negative and positive controls, respectively. Amounts of total RNA assayed are indicated above each lane. All three PARs are represented in embryonic and extraembryonic tissue at E9.5. Note the stronger relative expression of *Par1* mRNA in embryos versus yolk sacs. Alternatively, *Par3* and *Par4* mRNAs are more highly represented in yolk sacs than in embryos.

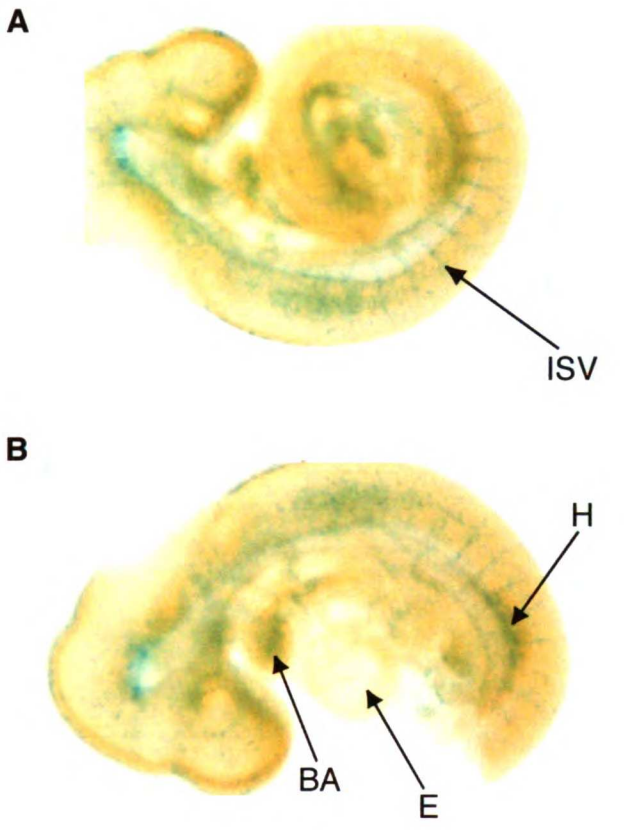

Fig. 11: PAR4 vascular expression at E9.5.
A: A homozygous PAR4-*lacZ*(neo-) knock-in embryo is shown after four days of staining in X-gal solution and subsequent clearing. The *lacZ* staining pattern reveals that PAR4 is primarily expressed in blood vessels at E9.5, in a pattern similar to that of PAR1 expression in endothelium at this time (see Chapter 4, Fig. 15). ISV=intersomitic vessel; 6.8x magnification. **B**: The embryo from (**A**) is exhibited with its tail removed to provide a clear view of the heart. Notice that the endocardium (E) is not noticibly stained, although the branchial arches (BA) stain strongly. Additionally, note the hindlimb (H) staining. 7x magnification.

A

	Par1+/+	*Par1+/-*	*Par1-/-*
Par4-/-	31	66	3

Live Offspring: 100 total

B

	Par4+/+	*Par4+/-*	*Par4-/-*
Par1-/-	17	35	5

Live Offspring: 57 total

Fig. 12: PAR4-deficiency augments *Par1-/-* embryonic lethality.
A: Live progeny of matings between *Par1+/-Par4-/-* parents. All offspring were genotyped by Southern analysis. Note the 88% embryonic lethality observed in the *Par1-/-Par4-/-* population ($0.001 >> p$ by Chi-square analysis against expected Mendelian numbers; $0.01 > p > 0.005$ by Chi-square analysis against 50% expected lethality based on historical analysis of *Par1-/-* embryonic lethality). Average litter size: 5.6. **B**: Live progeny of matings between *Par1-/-Par4+/-* parents. The small average litter size (3.8) is in keeping with the expected 50% lethality of PAR1-deficient offspring from these matings. The 65% embryonic lethality observed in the surviving *Par1-/-Par4-/-* offspring combined with presumed 50% lethality amongst all the progeny brings the total lethality of doubly-deficient mice from these matings to 82%. The data indicate that the combined loss of PAR1 and PAR4 signaling likely accounts for the 85-100% lethality observed in *TF-/-* and *Par1-/-FV-/-* embryos.

Chapter IV

PAR EXPRESSION PATTERNS DURING DEVELOPMENT: OTHER POTENTIAL ROLES FOR PROTEASE SIGNALING IN THE EMBRYO

ABSTRACT

Thrombin is an agonist for a variety of cellular responses in cultured cells. Agonist peptides have been utilized to attribute some of these responses to specific PARs *in vitro* and have illustrated the redundant expression patterns and functions of PARs in certain cell types [*21,61,64,65*]. Northern blots and *in situ* hybridization have provided additional information about PAR expression in adult mice and humans [*17,66*], but low levels of mRNA expression have complicated efforts at detailed cellular analysis of PAR expression during development [*27*]. Because of the embryonic lethality associated with loss of PAR1 and of PAR1/PAR4 function, we wanted to more accurately understand PAR expression patterns in the embryo. We utilized targeted insertion of the *LacZ* gene into PAR coding regions to report transcript expression in embryos and adult mice. This technique allowed us to describe a number of novel developmental expression sites of PARs and will potentially help us better understand functional overlap and specificity of the PARs in embryos and adults. Additionally, our PAR1-*LacZ* construct allowed us to analyze the phenotype of PAR1-deficient embryos in the absence of the PGK-NEO^R

cassette, thereby allowing us to rule out the possibility that the strong PGK promoter was affecting nearby gene expression (i.e. PAR2 and PAR3) and was complicating phenotypic analysis of our original *Par1* knock-out.

RESULTS

β-galactosidase produced by the *LacZ* gene from *E. coli* has been a useful reporter of gene expression in targeted mice [*67*]. β-galactosidase is a stable enzyme, and its expression does not appear to be either deleterious or advantageous to transgenic mammals [*68*]. In order to analyze sites of PAR expression during embryonic development, our lab made *LacZ* "knock-in" constructs for PARs1, 2, and 4. The PAR1-*LacZ* targeting vector (Fig. 13) was designed based on the successful expression of β-galactosidase in PAR2-*LacZ* targeted embryos from the lab. In each case, the *LacZ* gene carrying its own Shine-Dalgarno-Kozak sequence and a floxed PGK-Neomycin resistance casette were inserted in tandem in the same transcriptional direction as the gene of interest. The insertion replaced the ATG start site and a few subsequent codons of the first exon. An embryo or mouse with a successful targeting event should lose functional expression of the gene of interest while expressing β-galactosidase in a gene-specific manner. β-galactosidase, therefore, becomes a marker for sites at which the functional PAR should have been expressed.

The design of the PAR1-*LacZ* targeting vector provided a unique opportunity to confirm the phenotype of previously reported *Par1-/-* embryonic lethality [*20*]. The earlier vector targeted the PGK-neomycin resistance cassette to exon two of the *Par1* gene, replacing the gene segment encoding transmembrane domains 1-7. The PGK-NEO^R casette was not flanked by loxP sites ("floxed"), so phenotypic analysis was carried out in the presence of the cassette. The PAR1-*LacZ* vector targeted the β-galactosidase gene and floxed PGK- NEO^R cassette to exon one of *Par1* replacing the

start codon and codons 2-4 of the gene. Exon one encodes the 5' untranslated sequence and signal peptide of the receptor. Heterozygous PAR1-*LacZ* mice were mated to β-actin-*cre* mice [*69*] for excision of the PGK-NEO^R cassette, and two independent lines of mice were maintained—PAR1-*LacZ*(neo+) and PAR1-*LacZ*(neo-). Therefore, PAR1-*LacZ*-targeted mice provided the opportunity to analyze the effect of targeting the *Par1* gene in two functionally different regions and the effect of the PGK-NEO^R cassette on the partial lethality phenotype of *Par1-/-* embryos.

PAR1-*LacZ* heterozygous males and females were mated to assess embryonic lethality in the presence or absence of the PGK-NEO^R cassette, since this cassette has been shown to complicate phenotypic analysis of knock-outs by disrupting genes located near the intended target [*70*] (Fig. 14). The distribution of offspring from PAR1-*LacZ*(neo+) heterozygous parents was reminiscent of that seen with our original *Par1+/-* matings [*20*] ($0.01>p>0.005$ by χ^2 analysis when compared to an expected Mendelian distribution) (Fig. 14A). The lethality of PAR1-*LacZ(neo+)-/-* embryos was 56%--very statistically similar to the 50% lethality described with the two previously analyzed targeting vectors [*20,25*] ($0.975>p>0.9$ by χ^2 analysis). Heterozygous matings with PAR1-*LacZ*(neo-) mice also resulted in a distribution of offspring that was significantly different than the expected Mendelian distribution ($0.025>p>0.01$ by χ^2 analysis) (Fig. 14B). The lethality of PAR1-*LacZ(neo-)-/-* embryos was 63%--again statistically similar to the 50% lethality predicted by previous analysis of *Par1-/-* embryos ($.9>p>.5$ by χ^2 analysis). These results provided the first definitive proof that the PGK-NEO^R cassette does not contribute to the partial lethality of *Par1-/-* embryos.

The strong promoter for phosphoglycerate kinase (PGK), which is used to drive the neomycin resistance gene in our constructs, has also been shown to affect transcription of adjacent reporter genes [*71*]. For this reason, the PGK-NEO^R cassette is often flanked by *loxP* sites to enable removal of the cassette as a precaution against confounding analysis of reporter expression. In our own lab, for instance, β-galactosidase expression was not detectable in PAR2-*LacZ*-targeted embryos and adults until the PGK-NEO^R cassette was removed (unpublished observations of Mark Kahn and Yao Wu Zheng). Therefore, to assess the effects of the PGK promoter on *LacZ* transcription, we stained both PAR1-*LacZ*(neo+) and PAR1-*LacZ*(neo-)-targeted embryos for β-galactosidase activity. We found that β-galactosidase activity was much stronger in embryos containing the PGK-NEO^R cassette than in embryos in which the cassette had been excised. This phenomenon persisted throughout the developmental time points analyzed (E9.5-15.5). However, the enhanced staining patterns observed in PAR1-*LacZ*(neo+)-targeted embryos were distributed similarly to the reduced staining patterns seen in PAR1-*LacZ*(neo-)-targeted embryos.

At E9.5, the β-galactosidase staining pattern seen in PAR1-*LacZ*(neo+) heterozygous and homozygous embryos confirmed the predominantly endothelial pattern of PAR1 expression determined earlier by *in situ* hybridization experiments [*27*] (Fig. 15, B and C). This result was gratifying because it provided proof of the specificity of our targeted *LacZ* expression and validated the rescue of *Par1-/-* embryonic lethality achieved with the TIE2p/e-PAR1 transgene described in Chap. II. Furthermore, the detection of homozygous embryos with swollen pericardial cavities (Fig. 15B) provided proof that the embryonic lethality associated with PAR1-deficiency in the knock-in

construct recapitulated the phenotype of previously analyzed *Par1-/-* embryos. In addition to the β-galactosidase staining seen in embryonic endocardium and large vessel endothelium at E9.5, strong expression was also seen in a small minority of circulating blood cells, the mesenchyme of the hindlimbs, and a region of mesenchymal-appearing tissue caudal to the heart. The mesenchymal area below the heart appeared to encompass the septum transversum—the site of the future diaphragm. This region is closely associated with the sinus venosus where vascular defects occurred in some of our *Par1-/-* embryos (see Chapter 2, Fig. 2). Further histological analysis will help us determine more accurately whether the strong β-galactosidase staining observed in this area is mesenchymal or endothelial. Endothelial cells associated with developing liver vessels are evident in this region in TIE2-*LacZ* embryos at E9.5, but by comparison the staining seen in the PAR1-*LacZ*(neo+) embryos is more diffuse. β-galactosidase staining in the vasculature of PAR1-*LacZ*(neo-) heterozygous and homozygous embryos at E9.5 is too weak to detect after three days of incubation in X-gal solution at room temperature (Fig. 15A), so our knowledge of PAR1 expression at midgestation—the time of *Par1-/-* lethality—is primarily based on β-galactosidase expression in embryos containing the PGK-NEO^R cassette at the targeting site. However, the correlation between the β-galactosidase staining in the PAR1-*LacZ*(neo+)-targeted embryos and *in situ* hybridization for *Par1* mRNA at E9.5 supports the specificity of our *LacZ* expression in the presence of PGK-NEO^R.

PAR1 expression in embryonic vasculature diminshed between E10.5-11.5. By E10.5, the β-galactosidase staining in the PAR1-*LacZ*(neo+) heterozygous and homozygous embryos became weaker in the majority of embryonic blood vessels (Fig.

16, B and C). However, intersomitic vessels and endocardium were still visibly stained at this time (Fig. 16B). Staining intensified in the abdominal region (in particular, the septum transversum region) and hindlimbs. The homozygous PAR1-*LacZ*(neo-) embryo shown in Fig. 16A is phenotypically identical to affected *Par1-/-* embryos previously characterized at this time. Therefore, its staining pattern is more characteristic of an E9.5 embryo, which is presumably when it died from loss of functional PAR1. A significant upregulation of PAR1 expression occurred in the wall of the thoracic cavity and in the liver capsule by E11.5, while the endocardial expression previously observed was largely diminished (Fig. 16, D-F). The septum transversum region was still prominently stained, and the umbilical vessels strongly expressed PAR1 at this time (Fig. 16F). Lastly, the hindlimb expression, which had been ubiquitous at E10.5 (Fig. 16B), was restricted to the superior and lateral aspects of the region joining the hindlimb to the body by E11.5 (Fig. 16F).

The changes in PAR1 expression between E11.5-12.5 were minimal. Strong expression persisted in the wall of the thoracic cavity and in the liver capsule at E12.5 (Fig.17, A and B). Additionally, β-galactosidase staining was detected in the cartilage primordia of the developing ribs (Fig. 17A). Blood vessels were still visibly stained, although faintly, in the head (Fig. 17C). The lens of the eye was also consistently stained in PAR1-*LacZ*(neo+) homozygous embryos (Fig. 17C).

At E13.5, PAR1 expression intensified in previously identified sites and expanded to new sites (Fig. 18). For example, the staining in the superior aspect of the joint region of the hindlimb continued to be strong even in a PAR1-*LacZ*(neo-) uncleared embryo (Fig. 18A). In addition, new staining patterns appeared in the head (i.e. tongue) and in

the developing mammary glands (Fig. 18, A and B). The (neo+) homozygotes and heterozygotes expressed β-galactosidase at stronger levels than the (neo-) embryos, as usual, including sites in the brain. Staining was seen in clusters of cells found dorsal to the eye and rostral to the tongue in the heads of (neo+) and (neo-) embryos that will need to be more rigorously identified by histological examination (Fig. 18, B and F). One interesting staining discrepancy was noted in the tongue. While the homozygous (neo-) embryos—typically lower expressors than (neo+) heterozygotes or homozygotes—displayed strong tongue staining, comparable staining was not detected in any (neo+) embryos at this stage.

By E14.5 and E15.5, the β-galactosidase staining in the PAR1-*LacZ*(neo+) heterozygous and homozygous embryos became too superficial to enable detailed analysis of expression beneath the skin, even after clearing (Figs. 19 and 20). Further histological analysis of stained embryos at these stages will compensate for the lack of information gleaned from whole mount staining. The β-galactosidase staining in the PAR1-*LacZ*(neo-) heterozygous and homozygous embryos was more useful at these later embryonic stages because *LacZ* expression in the skin was not strong enough to obscure analysis of internal staining. At E14.5, staining in a homozygous (neo-) embryo was still visible in the tongue and in the wall of the thoracic/abdominal cavities (Fig. 19A). Interestingly, strong staining was observed in the intervertebral discs of a heterozygous (neo+) embryo when the skin was peeled away (Fig. 19C). As somite-derived sclerotome condenses, each sclerotome becomes subdivided into two portions: a caudal portion and a rostral portion with less condensation than the caudal portion. The condensed portion tends to migrate caudally and fuses with the rostral part of its immediate neighbor to form

the precartilaginous vertebral body, while the lower part of the less-condensed portion/upper part of the condensed portion differentiates to form the intervertebral disc [*72*]. Evidence of PAR1 expression in condensing sclerotome prior to the intervertebral disc expression at E14.5 was detected a day earlier at E13.5 (Fig. 18C). By E15.5, PAR1 was also detectable in the intervertebral discs of homozygous (neo-) embryos as well as in a stripe of expression along the ventral aspect of the tail (Fig. 20C). Furthermore, PAR1 was expressed on the caudal side of the genital tubercle in (neo-) embryos at this time (Fig. 20B). Superficial β-galactosidase staining was analyzed in (neo+) homozygous and heterozygous embryos, and one novel site of expression was the area surrounding (but not including) the whisker follicles (Fig. 20F). Staining of histological sections will provide more information about PAR1 expression in these late-stage embryos.

PAR1 is not the only protease-activated receptor with surprising developmental expression patterns. Our lab also made a PAR2-*LacZ* mouse that demonstrated strong β-galactosidase upon removal of the PGK-NEO^R cassette (unpublished results of Yao-Wu Zheng and Mark Kahn). PAR2 is activated by trypsin [*17*], tryptase [*18*], and coagulation factors VIIa and Xa [*19*], but not by thrombin. In adult mice, PAR2 is expressed in small intestine, stomach, kidney, and eye as determined by Northern analysis [*17*], but *Par2-/-* mice appear normal and have not yet elucidated our understanding of the receptor's *in vivo* roles. *Par2-/-* embryos survive development in a mixed C57Bl/6J-SV/129J background but are susceptible to partial lethality in a high percentage C57Bl/6J background (unpublished observations of Gilbert Sambrano). The cause of this embryonic lethality is not yet understood, and even a clear understanding of the time of death has been elusive (E12.5-E18.5). At face value, the phenotype appears

to be one of failed hematopoiesis since the dead embryos are pale and without evidence of hemorrhage. Further analysis of the phenotype and pursuit of the modifier responsible for its appearance are being performed in the lab.

PAR2 expression during development, as determined by β-galactosidase staining of PAR2-*LacZ*(neo-) heterozygous and homozygous embryos, was evident as early as E8.5. From E8.5-E9.5 the receptor appeared to be primarily restricted to the neural fold of the developing embryo (Fig. 21, A and B). While at E8.5 the receptor was expressed along the entire length of the neural fold, by E9.5 the expression was restricted to the caudal end of the fold. By E12.5, PAR2 was most strongly expressed in the olfactory epithelium of the nasal cavity and in the hip region of the hindlimb (Fig. 21, C and D). Staining was seen to a lesser extent in the shoulder region. One day later, at E13.5, expression began to appear in the whisker follicles and to expand to skeletal muscle in the shoulder region (Fig. 22, A and B). Additionally, PAR2 was expressed in the mammary gland primordia and in the condensing sclerotome of the developing intervertebral discs. Expression in the hip region was still strong at E13.5 and maintained a horseshoe pattern along the ventral and lateral aspects of the hip (Fig. 22C). By histology, this expression in the hip region was superficial, although distinctly underlying the epidermis, and was confined to cells of mesenchymal appearance (not shown). Histological examination of the expression pattern in the nasal cavity revealed staining in a subset of olfactory epithelium at the distal-most portion of the nasal turbinates (Fig. 22D). At E15.5, PAR2 expression persisted in the previously described locations and expanded to all the hair follicles of the body, the eyelids, between the digits of the forelimbs and hindlimbs, and into additional skeletal muscle in the neck and chest (Fig.

23, A-C). Additionally, PAR2 expression in the intervertebral discs at this time was impressively strong and was restricted to the outer annulus of each disc (Fig. 23, D-F). The outer annulus of the mature disc consists of a number of oriented collagenous lamellae, which are laid down by criss-crossed sheets of fibroblasts (as seen in Fig. 23F) [*73*]. In the adult, these lamellae provide the disc with strength during bending and twisting. Overall, PAR2 and PAR1 developmental expression overlapped in the hip region, the intervertebral discs, the mammary gland primordia, and the whisker follicle region (PAR1 surrounded the follicles while PAR2 was located in the follicles themselves). Such overlapping expression may speak toward a functional redundancy that could be detected with doubly-targeted PAR1/PAR2-deficient mice.

Embryonic expression of PAR3 and PAR4 has not yet been carefully explored primarily because *Par3-/-* and *Par4-/-* embryos survive development without lethality. Our lab has not made a PAR3-*LacZ* knock-in mouse at this time. PAR3 is strongly expressed in megakaryocytes of the adult mouse by *in situ* hybridization, and *Par3-/-* mice elucidated the receptor's role in platelet activation at low concentrations of thrombin [*16*]. Surprisingly, PAR3 has not been shown to function independently in the mouse, although co-expression of mPAR3 with mPAR4 reliably enhances both mPAR4 cleavage and signaling at low concentrations of thrombin compared with mPAR4 alone [*23*]. The exclusivity of mPAR3's cofactoring role for PAR4 *in vivo* has not been determined. By *in situ* hybridization, PAR3 mRNA is expressed in liver and gut at E14.5, which is a similar expression pattern to that of PAR4 as detected by β-galactosidase staining of PAR4-*LacZ*(neo-) embryos at this time (unpublished observations of Yoga Srinivasan and Yao Wu Zheng, respectively). Perhaps these

overlapping expression patterns of PAR3 and PAR4 at E13.5 are indicative of their co-factoring roles in development. However, it is possible that PAR3 can signal independently during development. Our lab has made a PAR4-*LacZ* mouse that expresses *LacZ* upon removal of the PGK-NEO^R cassette [*24*]. PAR4-*LacZ*-targeted embryos have not yet been thoroughly analyzed for β–galactosidase expression throughout development, although expression appeared vascular at E9.5 (see Chapter 3, Fig. 11) and appeared restricted to gut and liver at E13.5 (unpublished observations of Yao Wu Zheng).

DISCUSSION

Our finding of similar phenotypes in our homozygous PAR1-*LacZ*(neo-) embryos and the original *Par1-/-* embryos was an important demonstration of the accuracy of our original phenotypic analysis. PAR1, PAR2, and PAR3 are located in a cluster on mouse chromosome 13D2 that spans 80 kb [*74*]. Confounding phenotypes of knock-outs from multigenic families due to the presence and direction of the PGK-NEO^R cassette in targeting constructs have been previously reported [*70*]. Given the proximity of the PARs on chromosome 13 to one another and the redundancy of their developmental expression patterns demonstrated in *LacZ* knock-in embryos, we realized the importance of determining whether the developmental effects of PAR1-deficiency were due to loss of PAR1 function or were due to alteration of functions of nearby genes such as PAR2 or PAR3. By removing the PGK-NEO^R cassette from targeted PAR1-*LacZ* mice, we were able to determine with confidence that the embryonic *Par1-/-* phenotype described in Chapter II is specifically due to PAR1-deficiency.

Analysis of *LacZ* knock-in embryos has revealed a number of novel sites of potential protease signaling during development (Table 2). While *Par1-/-* embryos have a definitive midgestational phenotype that provides independent evidence of the receptor's importance in development, *Par2-/-*, *Par3-/-*, and *Par4-/-* embryos have no detectable developmental phenotypes, despite high levels of expression detected by β–galactosidase staining and by *in situ* hybridization in our lab. It is possible that loss of receptor function in some of the novel expression sites described in this chapter results in phenotypes too subtle to be detected by gross analysis. For example, *Par2-/-* mice may

be unable to smell particular odors due to loss of receptor function in olfactory epithelium. Additionally, the overlap of PAR expression seen in certain developmental tissues raises the possibility that redundant protease signaling masks the phenotypic effects of single PAR knock-outs. Multiple PAR knock-outs are currently being generated by our lab to help reveal potential phenotypes at these sites of overlapping expression.

The redundancy of PAR expression at particular sites and times of development may indicate that conserved promoter elements are shared between some or all of the PARs. *Par1* and *Par2* are thought to have arisen from a gene duplication event that occurred relatively recently in the history of the gene family [*74*]. Duplication of promoter elements driving, for example, intervertebral disc expression of *Par1* and *Par2* could explain their tightly coordinated expression in that tissue. Alternatively, it's possible that another neighboring gene with its own strong promoter could drive β-galactosidase expression from the PAR1-*LacZ* and PAR2-*LacZ* constructs. Such an effect is best illustrated by our differing levels of β-galactosidase expression in (neo+) versus (neo-) PAR1-*LacZ* embryos; in this case the PGK promoter attached to the NEO^R cassette clearly enhanced β-galactosidase expression—albeit in a manner that was specific for sites of endogenous PAR1 expression. *In situ* hybridization data from our lab provide evidence against this hypothesis, since wildtype *Par1* and *Par2* mRNAs are seen in the intervertebral discs of late-gestational embryos. It would be interesting, therefore, to search the mouse genomic database for promoter elements shared between *Par1* and *Par2* that might promote expression in shared sites such as the intervertebral discs and hip. It would also be interesting to assess whether PAR3—which resides on the same

locus with PAR1 and PAR2—is expressed at sites redundant with the first two receptors. Does PAR3 share the promoter elements that drive PAR1 and PAR2 in the intervertebral discs and hip regions? Preliminary *in situ* hybridization data indicate that this might not be the case—the receptor appeared to be primarily expressed, like PAR4, in the gut and liver at E13.5, (unpublished data of Yoga Srinivasan).

What do the expression sites revealed in PAR1-*LacZ* embryos beyond midgestation tell us about the receptor's function? We found PAR1 in such varied and unexpected places as the body wall, liver capsule, and tongue by E13.5. This varied expression pattern indicates that the receptor may be signaling different functions at different sites (i.e. proliferation, migration, or the induction of apoptosis). Perhaps the most interesting question raised by such diverse sites of expression is whether thrombin or some other protease is activating the receptor at these sites. These and other sites of expression shared with PAR2 (the mammary gland primordia, intervertebral discs, and mesenchyme underlying the epidermis in the hip region) are all removed from the blood and circulating coagulation factors. It seems likely, then, PAR1 and PAR2 can respond to novel proteases—and perhaps even the same protease at sites of overlapping expression—during development to achieve intracellular signaling.

Although PAR2, like PAR1, is also expressed in seemingly unrelated sites in the embryo (olfactory epithelium and skeletal muscle), the receptor might participate in a more unified function during late development. Many of the sites of PAR2 expression at E15.5 are found at epithelial/mesenchymal borders (i.e. the eyelid, hair follicles, between the digits, the ear canal, the developing mammary glands, and the mesenchymal tissue below the epidermis of the hip). Epithelial-mesenchymal interactions are well

characterized for their roles in secondary induction events in which the mesenchyme instructs epithelium in its cellular differentiation (to hair, feathers, skin, etc.) [*75*]. According to the β-galactosidase staining seen in the PAR2-*LacZ* knock-in embryos, PAR2 is uniquely positioned to participate in such differentiation events at a number of sites. Again, the question of what protease(s) serves as a ligand for the receptor at epithelial/mesenchymal borders is perplexing. Certainly a search for developmental ligands for PAR1 and PAR2 will be instructive in our understanding of PAR signaling and biology.

Overall, the *LacZ*-targeted embryos provide several surprising pieces of information about PAR1 and PAR2 expression during development. For example, although PAR1 is highly and predominantly expressed in the vasculature at midgestation, by E12.5 its vascular expression is much weaker than its expression in unexpected sites such as the tongue, hindlimbs, and intervertebral discs. Eventually, multiple PAR knock-outs may reveal phenotypes that substantiate our findings of overlapping expression patterns. In the meantime, the *LacZ* knock-in embryos will continue to direct our attention to novel tissues and organs in our effort to understand the biology of protease signaling during development.

METHODS

PAR1-*LacZ* knock-in targeting vector. The start ATG and codons 2-4 of *Par1* exon 1 were replaced with a *LacZ*-PGK-NEO^R cassette. The *LacZ*-PGK-NEO^R cassette was derived from pNTK [*76*] and was modified by insertion of tandem loxP sites [*77*] 5' and 3' to the PGK-NEO^R cassette and by subsequent insertion of the bacterial *LacZ* gene (without a poly-adenylation tail) 5' to the floxed PGK-NEO^R cassette in the same transcriptional direction. A Shine-Dalgarno-Kozak sequence immediately preceded the *LacZ* gene. A bacterial artificial chromosome (BAC) from a 129/SvJ mouse genomic library (Genome Systems) was used as a source of *Par1* DNA [*74*]. The 1320 bp short arm of the targeting vector was inserted between the PGK-thymidine kinase (TK) cassette and the 5' end of the *LacZ*-PGK-NEO^R cassette and was obtained by PCR of the BAC DNA with the following primers: forward 5'-ATGCGCGGATCCGTGATTGATGGGGAAAGGTCC and reverse 5'-ATACATGCATGCTGTCCCAAGGCTGCCCGCGCG. To generate a template for amplification of the long arm, a 5 kb *NotI/NcoI* fragment beginning 335 bp upstream of exon 1 and extending into intron 1 was subcloned from the BAC into a pET28 vector. PCR amplification of the 4.5 kb long arm utilized the following primers: forward 5'-ATACATAAGCTTCGCTTGCTGATCGTCGCCCTC and reverse 5'-ACGGTACTCGAGGAGATATACCATGGCTGGAAT. This fragment, which extended from 13bp downstream of the ATG start site of exon 1 into intron 1, was inserted at the 3' end of the PGK- NEO^R cassette to generate the final targeting construct. A unique *XhoI* site from the finished targeting vector was used for linearization of the construct.

RF8 ES cells [*78*] (129/SvJae) were electroporated with the linearized targeting construct. Clones resistant to G418 and FIAU were selected [*76*] and screened by Southern analysis. A 509 bp probe 5' of the short arm (i.e., outside of the targeting construct) was generated for Southern analysis by PCR of the BAC with the following primers: forward 5'-TAGCCTGGAGTTCGCTGAGTA and reverse 5'-ATGGTTGTGAACCACTGTGTG. Southern analysis of *HincII* genomic digests with this probe yielded 4.5 and 5.0 kb bands for the targeted and wild-type alleles, respectively. Four highly chimeric male mice derived from two different PAR1-*LacZ*+/- ES cell clones were bred to C57Bl/6 females to generate F1 *Par1*+/- mice. In vivo *cre*-mediated excision of the floxed NEO^R cassette was accomplished by mating β-actin-*cre* transgenic mice [*69*] (kind gift of Gail Martin) to PAR1-*LacZ*+/- mice. Excision was confirmed by Southern analysis using a probe against the NEO^R cassette.

LacZ staining, clearing, and histology. Whole embryos were dissected free of maternal tissue and were fixed in 2% paraformaldehyde/0.2% glutaraldehyde. Embryos were rinsed in PBS and stained overnight at room temperature in X-gal solution (5μM Potassium Ferricyanide, 5μM Potassium Ferrocyanide, 2μM $MgCl_2$, 1mg/ml X-gal in PBS). For embryos at E14.5 and E15.5, 0.02% NP-40, 0.01% Sodium Deoxycholate, and 20mM Tris (pH 7.4) were added to the staining solution. Blue embryos were washed in PBS and post-fixed in 4% paraformaldehyde. After post-fixation, some embryos were processed in plastic, sectioned (8μM), and stained with nulcear fast red. For clearing, post-fixed embryos were dehydrated through an ethanol series (25%, 50%, 75%, and 100% EtOH) for 10 minutes at each step. Subsequently, the embryos were passed through several changes of 100% methanol. Embryos were then placed in a clearing

solution of 50% benzyl alcohol-50% benzyl benzoate in a glass container until the embryos settled and cleared sufficiently for photography.

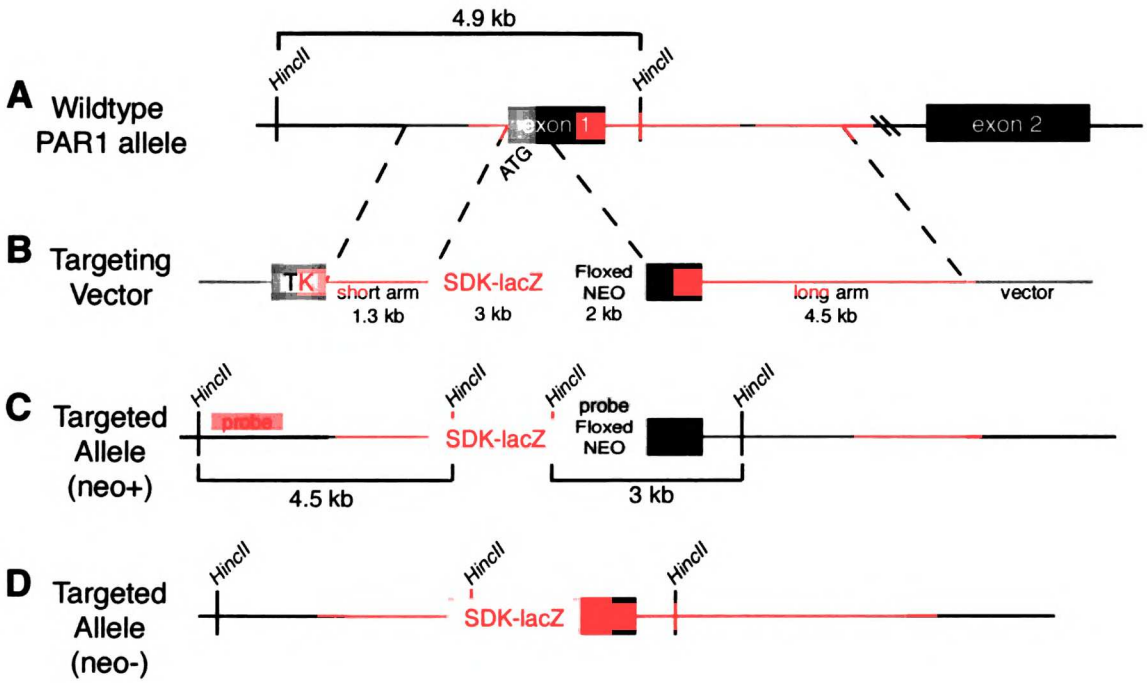

Fig. 13: PAR1-*LacZ* targeting construct.
The structure of the *Par1* gene (**A**) and targeting vector (**B**) are shown. The targeting vector contains a SDK-*lacZ*/PGK-neomycin resistance cassette, which replaces the start site and first three codons of murine exon 1, flanked by ~5.8 kb total homologous 5' and 3' arms. The PGK-NEO cassette is flanked by loxP sites ("floxed"). The predicted product of successful recombination is shown in **C**. The location of a probe (shown in orange), 5' of the short arm, used to detect successful targeting, is indicated. The targeted allele carries an additional *HincII* site within the SDK-*LacZ* cassette, allowing for identification of a 4.5 kb targeted allele versus 4.9 kb endogenous allele when genomic *HincII* digests are analyzed by Southern hybridization. Additionally, *HincII* digests can be hybridized with a probe (shown in pink) corresponding to the NEO cassette, which identifies a 3 kb fragment. A targeted allele in which the floxed NEO cassette has been removed by a *cre* recombinase is shown in **D**. The absence of a 3 kb band on a *HincII* Southern blot probed with the pink NEO probe shown in **C** is indicative of successful removal of NEO.

A

PAR1-*LacZ* (neo+):

WT	HET	KO
39 22 male 17 female	72 40 male 32 female	17 11 male 6 female

B

PAR1-*LacZ* (neo-):

WT	HET	KO
19 8 male 11 female	43 23 male 20 female	7 6 male 1 female

Fig. 14: Progeny from heterozygous PAR1-*LacZ* crosses.
A: Offspring of matings between PAR1-*LacZ*(neo+)+/- parents. Homozygous offspring are represented at 44% of their expected numbers. The distribution of progeny is significantly different than that predicted by Mendelian genetics ($0.01>p>0.005$ by Chi-square analysis). However, the distribution of progeny is not significantly different than that predicted if 50% of homozygous embryos die at midgestation as previously described for *Par1-/-* embryos ($0.975>p>0.9$ by Chi-square analysis). **B**: Offspring of matings between PAR1-*LacZ*(neo-)+/- parents. Homozygous offspring are represented at 37% of their expected numbers. As with the (neo+) embryos in **A**, the distribution of progeny from these crosses was significantly different than that predicted by Mendelian genetics but insignificantly different than that predicted by 50% *Par1-/-* lethality ($0.025>p>0.01$ and $0.9>p>0.5$, respectively, by Chi-square analysis). Note that the unequal numbers of male and female homozygotes from both crosses are not statistically significant.

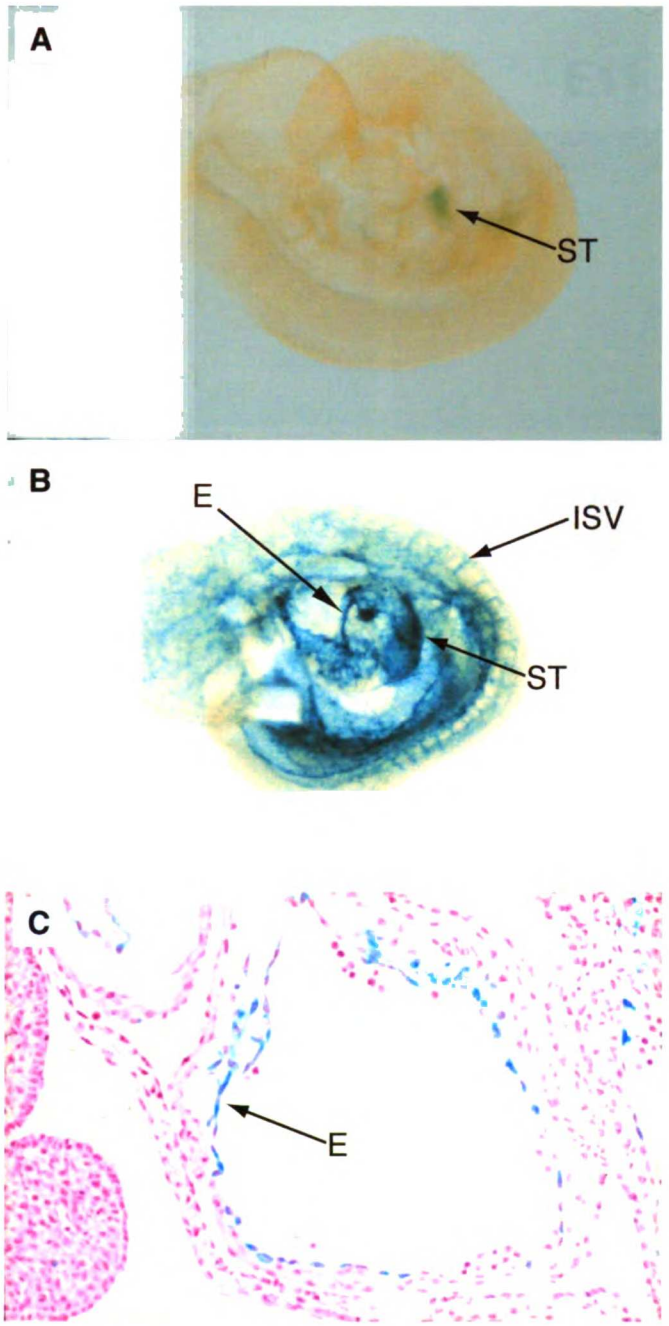

Fig. 15: PAR1 expression at E9.5.
A: A homozygous PAR1-*LacZ*(neo-) embryo stained for three days and cleared. The only visible staining is in the septum transversum (ST) region. 5.5x magnification. **B**: A homozygous PAR1-*LacZ*(neo+) with a swollen pericardial cavity characteristic of affected *Par1-/-* embryos. This embryo was stained overnight and cleared. E=endocardium, ISV=intersomitic vessel. **C**: A histological section of the heart from the embryo in **B** shown at 20x magnification.

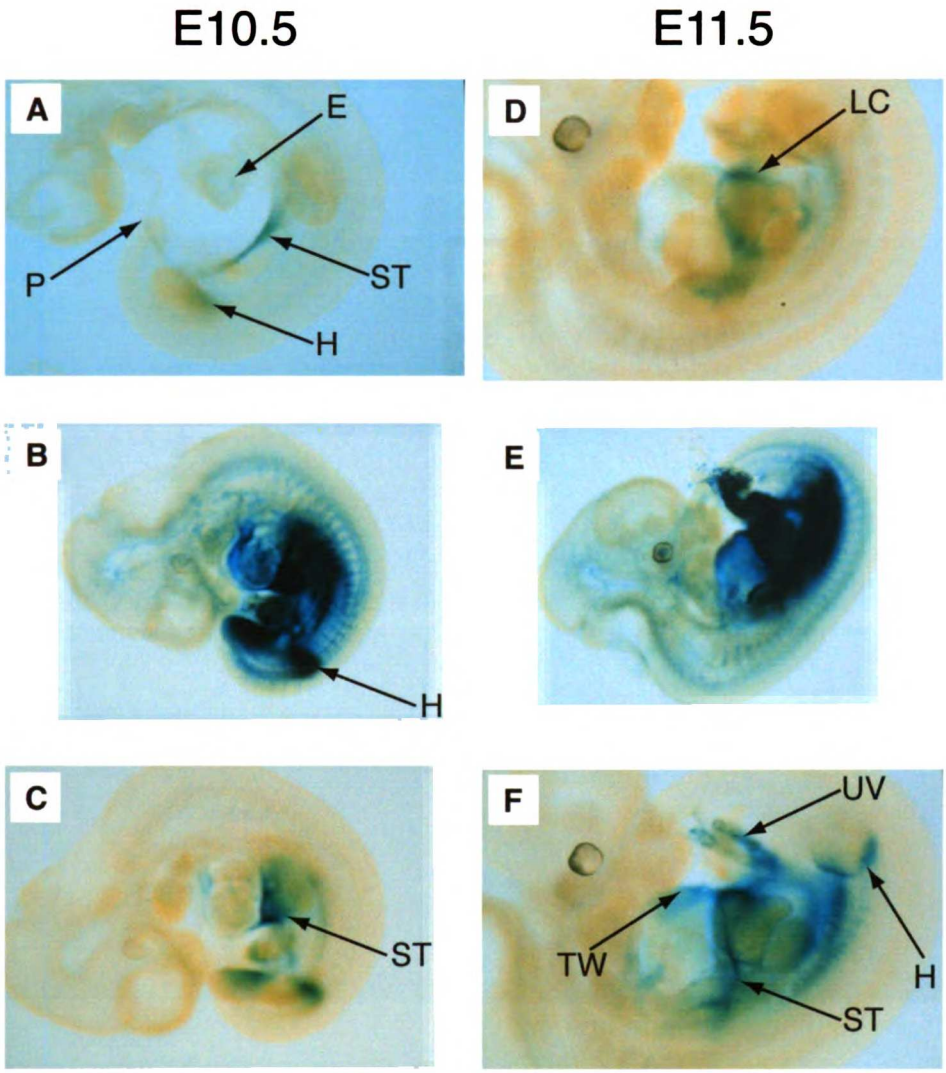

Fig. 16: PAR1 expression at E10.5-E11.5.
A-C: PAR1 expression at E10.5. **A**: A homozygous PAR1-*LacZ*(neo-) embryo with some developmental delay and a swollen pericardium (P). The staining is probably more representative of expression at E9.5 based on the phenotype. E=endocardium, ST=septum transversum region, H=hindlimb; 5x magnification; overnight staining. **B**: A homozygous PAR1-*LacZ*(neo+) embryo. 2.9x magnification; overnight staining. **C**: A heterozygous PAR1-*LacZ*(neo+) embryo with staining levels intermediate between (**A**) and (**B**). 3.1x magnification; overnight staining. **D-F**: PAR1 expression at E11.5. **D**: A homozygous PAR1-*LacZ*(neo-) embryo. LC=Liver capsule, 4x magnification; stained two days **E**: A homozygous PAR1-*LacZ*(neo+) embryo. 2.25x magnification; overnight staining. **F**: A heterozygous PAR1-*LacZ*(neo+) embryo. UV=umbilical vessel, TW=thoracic wall; 4x magnification; overnight staining.

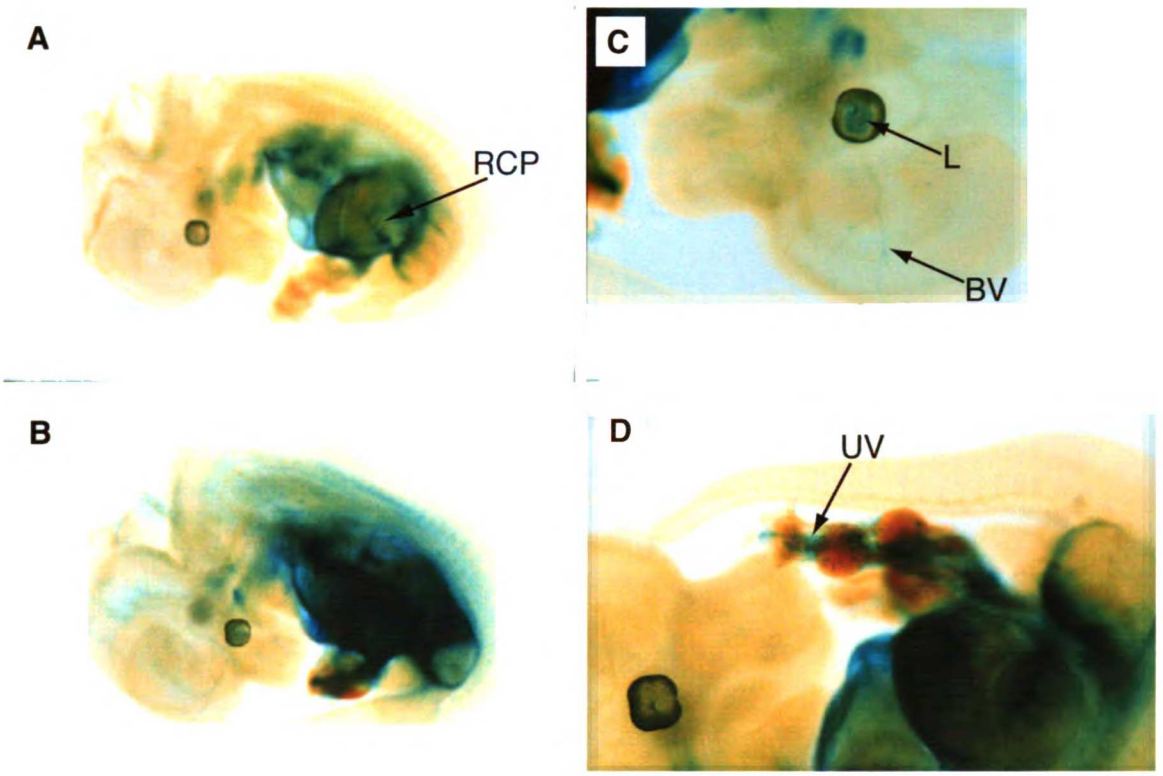

Fig. 17: PAR1 expression at E12.5.
A: A homozygous PAR1-*LacZ*(neo-) embryo. RCP=rib cartilage primordium; 2x magnification. **B**: A homozygous PAR1-*LacZ*(neo+) embryo. 2x magnification. **C**: A closer view of the head of the embryo shown in **B**. BV=blood vessel; L=lens; 4x magnification. **D:** A heterozygous PAR1-*LacZ*(neo+) embryo. UV=umbilical vessel; 4x magnification. All embryos were stained overnight and cleared.

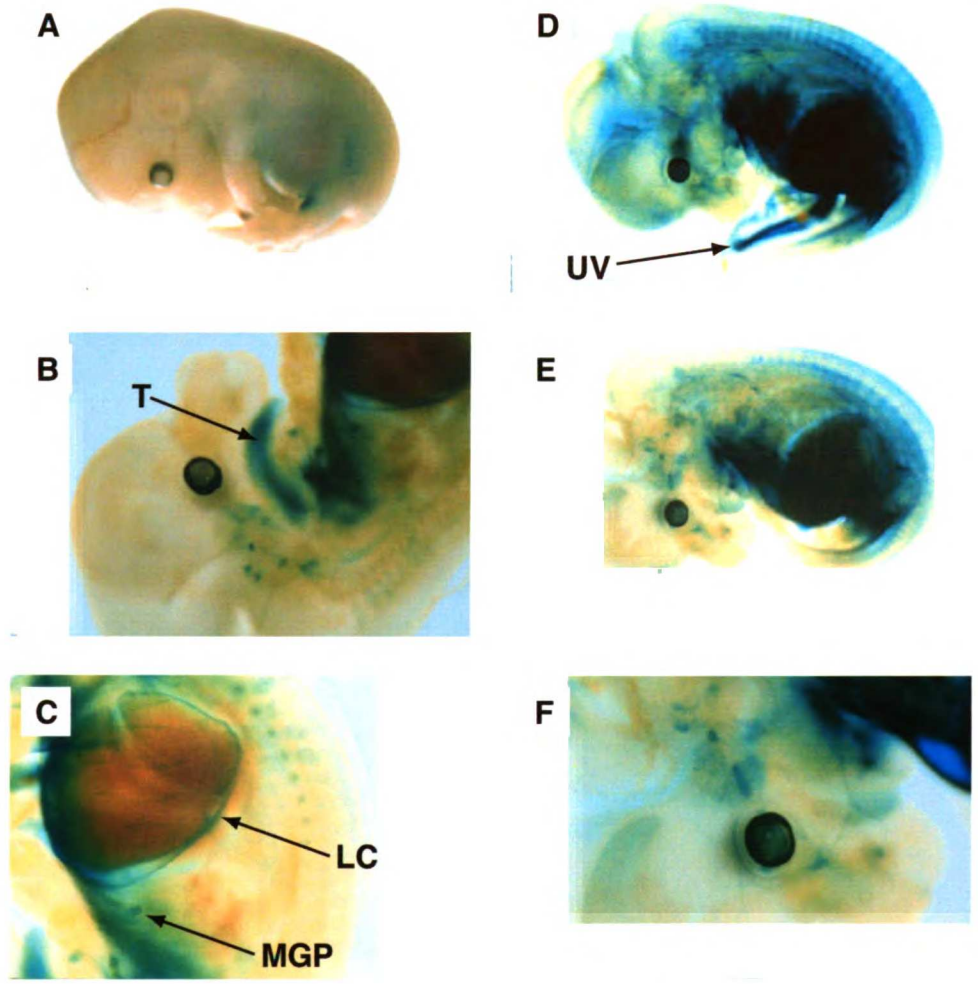

Fig. 18: PAR1 expression at E13.5.
A: A homozygous PAR1-*LacZ*(neo-) embryo stained for two days and photographed before clearing; 1.5x magnification. **B**: A view of the embryo shown in **A** after clearing. T=tongue; 2.5x magnification. **C**: A closer view of the abdominal region of the embryo shown in **A** and **B**. MGP=mammary gland primordium, LC=liver capsule; 3.1x magnification. **D**: A homozygous PAR1-*LacZ*(neo+) embryo stained overnight and cleared. UV=umbilical vessel; 1.75x magnification. **E**: A heterozygous PAR1-*LacZ*(neo+) embryo stained overnight and cleared. 1.75x magnification. **F**: A closer view of the head of the embryo shown in **E**. Note the decreased staining of the tongue compared to the (neo-) embryo shown in **B**. 3.5x magnification.

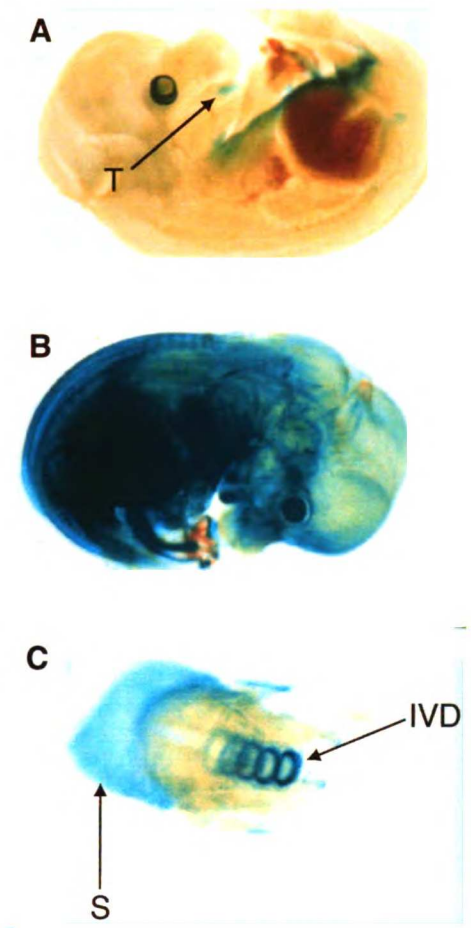

Fig. 19: PAR1 expression at E14.5.
A: A homozygous PAR1-*LacZ*(neo-) embryo. T=tongue; 1.5x magnification. **B**: A homozygous PAR1-*LacZ*(neo+) embryo. Superficial expression is too strong to allow for detailed analysis of internal organs. 1.5x magnification. **C**: A piece of tail with the overlying skin (S) peeled back from a heterozygous PAR1-*LacZ*(neo+) embryo. IVD=intervertebral disc; 5x magnification. All embryos were stained overnight and cleared.

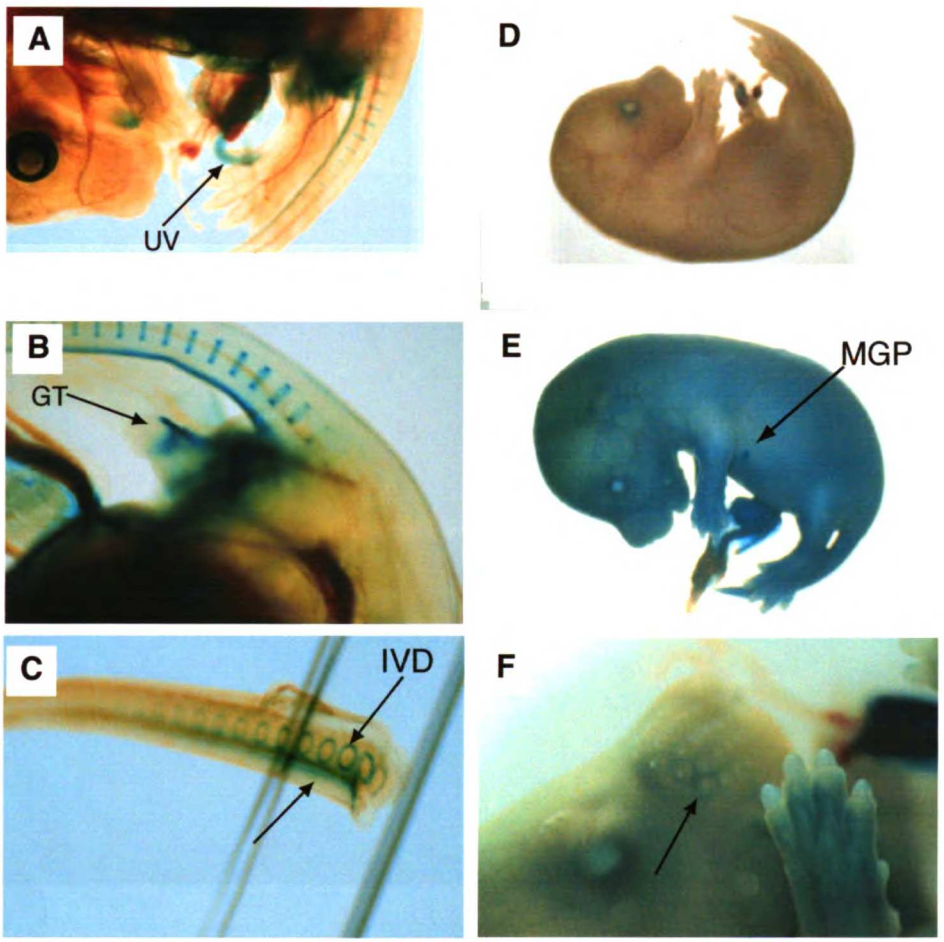

Fig. 20: PAR1 expression at E15.5.
A: A homozygous PAR1-*LacZ*(neo-) embryo. UV=umbilical vessel; 2x magnification. **B**: A homozygous PAR1-*LacZ*(neo-) embryo with its hindlimb removed for a clear view of the genital tubercle (GT). **C**: A closer view of the tail from the embryo in **A**. Note the intervertebral discs (IVD) and the stripe of PAR1 expression on the ventral side of the tail (arrow). 3.7x magnification. **D**: An uncleared wildtype embryo. 0.8x magnification. **E**: An uncleared homozygous PAR1-*LacZ*(neo+) littermate of the embryo in **D**. Staining is superficial, but the mammary gland primordia (MGP) are easily recognizable. 1x magnification. **F**: An uncleared heterozygous PAR1-*LacZ*(neo+) embryo with staining surrounding the whisker follicles (arrow). The embryos in **A-C** were stained overnight; the embryos in **D-F** were stained for two days.

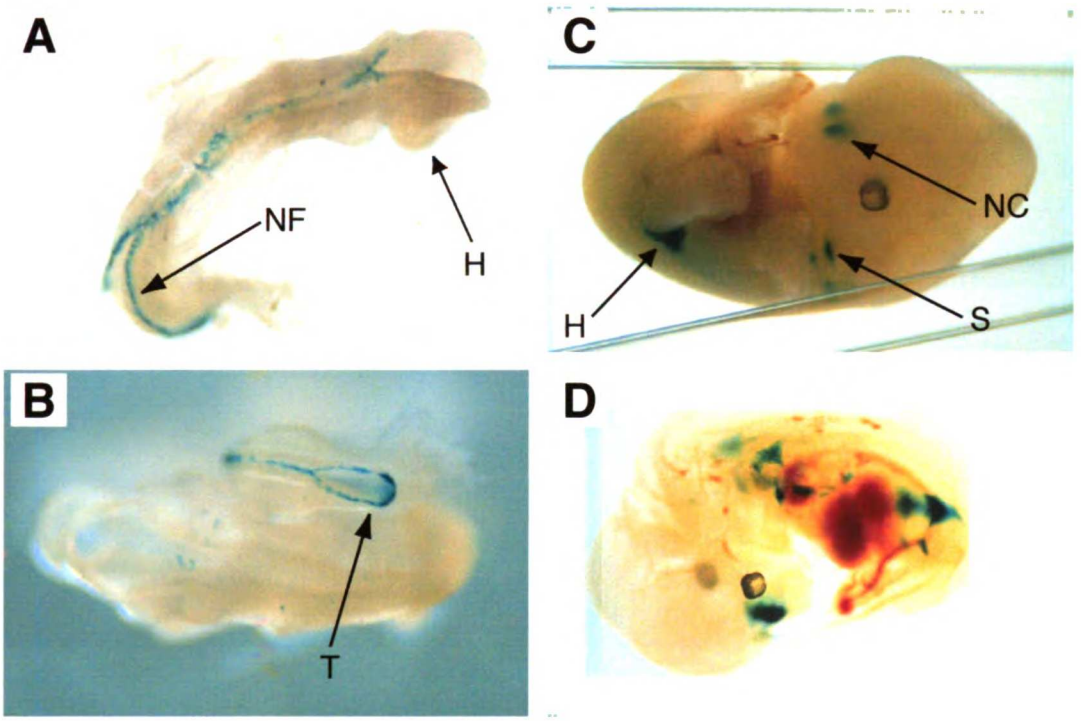

Fig. 21: PAR2 expression at midgestation.
A: A PAR2-*LacZ* embryo at E8.5; dorsal view. Expression is visible in the neural fold (NF). H=head. **B**: A PAR2-*LacZ* embryo at E9.5; dorsal view. PAR2 is still expressed in the neural fold at the caudal extreme of the embryo. T=tail. **C**: An uncleared heterozygous PAR2-*LacZ* embryo at E12.5. PAR2 is found in epithelial cells of the nasal cavity (NC) and in the hip (H) and shoulder (S) regions. **D**: The embryo shown in **C** after clearing. All embryos were stained overnight.

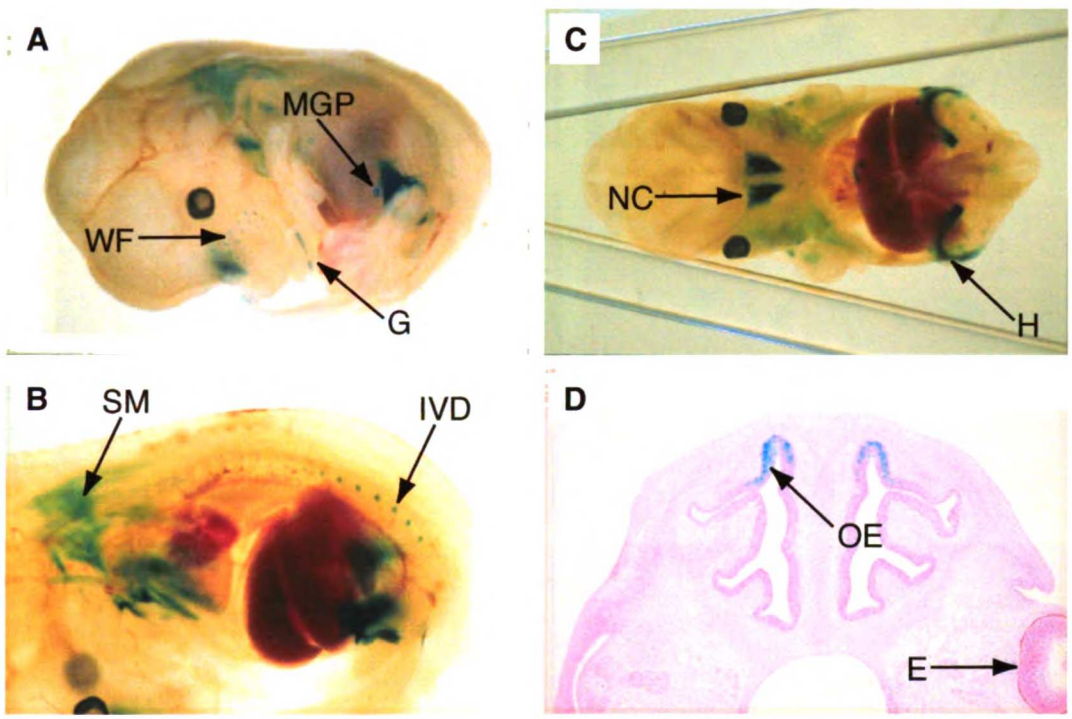

Fig. 22: PAR2 expression at E13.5.
A: An uncleared heterozygous PAR2-*LacZ* embryo. WF=whisker follicles, MGP=mammary gland primordium, G=gut loop. **B**: The embryo shown in **A** after clearing. The intervertebral discs (IVD) are at an early stage of formation. SM=skeletal muscle. **C**: Frontal view of the embryo shown in **B**. Note the superior and lateral expression of PAR2 in the hip region (H). NC=nasal cavity. **D**: A transverse section of the head of a heterozygous PAR2-*LacZ* embryo. Expression is consistently seen in the olfactory epithelium (OE) at the most distal end of the nasal cavity. E=eye; 4x magnification.

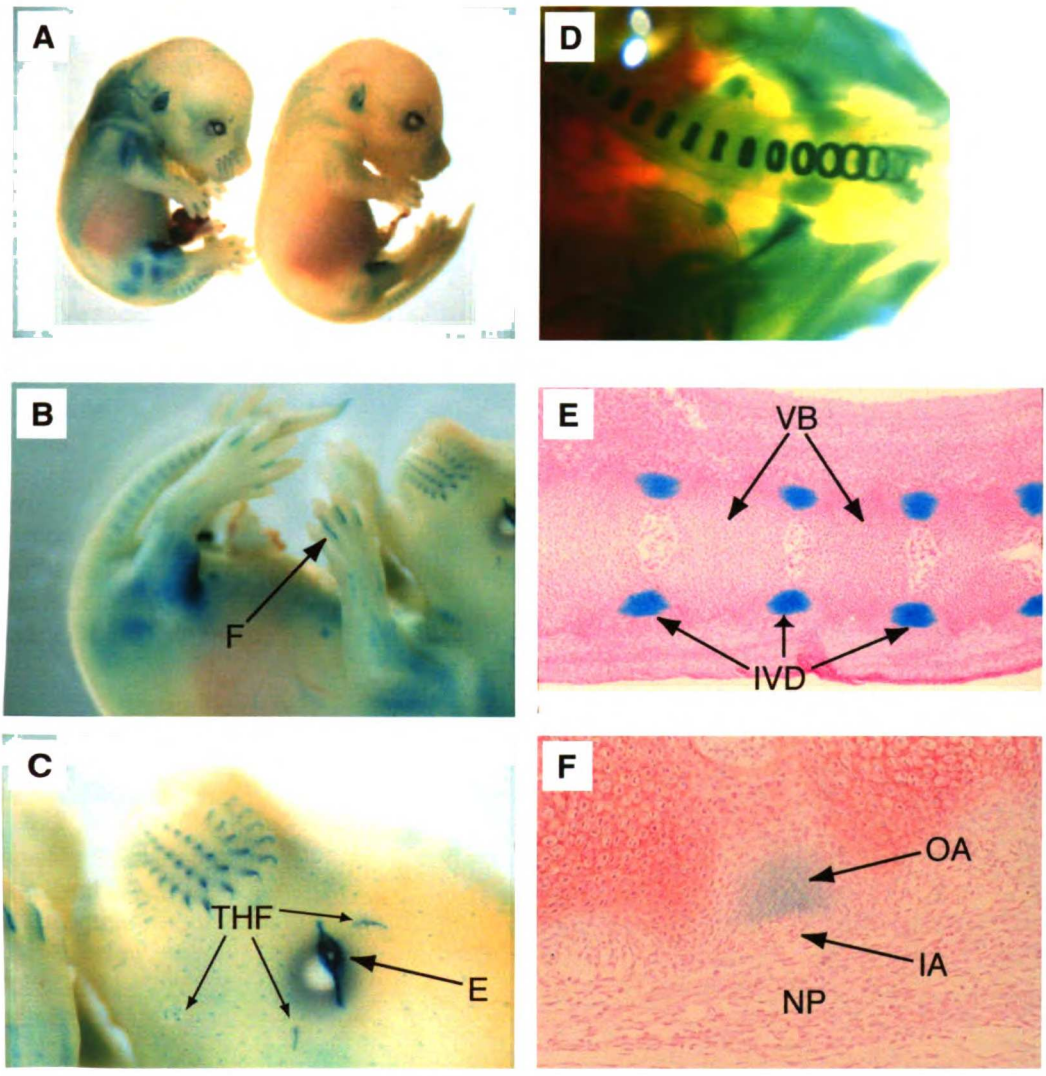

Fig. 23: PAR2 expression at E15.5.
A: PAR2-*LacZ* homozygous (left) and heterozygous (right) littermates before clearing. **B**: A heterozygous PAR2-*LacZ* embryo. PAR2 is expressed between the fingers (F) and toes of the forelimbs and hindlimbs. **C**: A closer view of the face of the embryo shown in **B**. The fusing eyelid (E) and tactile hair follicles (THF) express PAR2. **D**: A view of the tail of a cleared heterozygous PAR2-*LacZ* embryo. Note the rings of PAR2 expression in the intervertebral discs. **E**: A transverse section of the tail of a heterozygous PAR2-*LacZ* embryo. VB=vertebral bodies, IVD=intervertebral discs; 10x magnification. **F**: A closer view of an intervertebral disc from the tail section shown in **E**. PAR2 is expressed in the fibroblasts of the outer annulus (OA), which are characteristically arranged in sheets that lie 90° to one another. IA=inner annulus, NP=nucleus pulposus; 20x magnification. All embryos were stained overnight.

Tissue	E8.5	E9.5	E10.5	E11.5	E12.5	E13.5	E14.5	E15.5
Neural Fold	2	2						
Endothelium		1,4	1	1	1	1	1	1
Endocardium		1	1					
Umbilical Vessels		1	1	1	1	1	1	1
Septum Transversum		1	1					
Thoracic Wall				1	1	1	1	1
Liver Capsule				1	1	1		
Liver Cells							4	
Gut						2	4	2
Hindlimb		1,4	1,4	1				
Hip Region				1	1	1	1	1
Rib Cartilage Primordia					1			
Skeletal Muscle						2		2
Mammary Gland Primordia						1,2	1	1,2
Brain				1	1	1	1	1
Eye				1	1	1	1	1
Eyelid								2
Olfactory Epithelia					2	2		2
Tongue					1	1	1	1
Ear								2
Condensing Sclerotome						1,2		
Intervertebral Discs							1	1,2
Genital Tubercle								1
Whisker Follicles						2		1,2
Hair Follicles								2
Between Digits								2
Skin								1

Table 2: Sites of PAR expression during development. PAR1-*LacZ*(neo+)/(neo-)=(1), PAR2-*LacZ*(neo-)=(2), and PAR4-*LacZ*(neo-)=(4) embryos were X-gal stained for detection of β-galactosidase activity. Note that the data in this table only represent positive staining information; lack of representation of a PAR at any given time point may indicate lack of data rather than lack of expression. See Chapter 4 (results) for more detailed descriptions of expression sites.

Chapter V

FUTURE DIRECTIONS

This thesis describes the beginning stages of our lab's analysis of the role of protease signaling in the developing embryo. There are several avenues for expansion of the work described in the preceding chapters that will be critical in rounding out our knowledge of what PARs accomplish during embryogenesis.

In Chapter II we described the phenotype of *Par1-/-* embryos. Half of PAR1-deficient embryos bleed to death due to defective vascular integrity and can be rescued by restoring receptor expression to endothelial cells. A critical goal for the future is to understand the mechanism by which PAR1 signaling on endothelial cells during development prevents hemorrhage. We believe that embryonic endothelium in *Par1-/-* embryos develops holes large enough for blood to leak into extravascular spaces, but we do not know if PAR1 prevents holes from forming or if PAR1 prevents excessive bleeding through holes that arise independently. As discussed in Chapter II, thrombin is known to cause a number of changes in cultured endothelial cells including alterations in shape, motility, and proliferation (Table 3). We want to understand which of these changes is critical for hemostasis and/or vascular integrity during development. Likewise, a growing number of knock-outs have revealed deficiencies in midgestational vascular development (i.e. VEGF [*79,80*], the VEGF receptors [*81-83*], angiopoietin-1 [*84*], and the TIE receptors [*85*]), perhaps indicating the convergence of one or more of these signaling pathways with that of PAR1. One tool we can use to answer some of these questions is primary endothelium from our *Par1-/-* mice. Our lab has begun to

successfully culture such cells from *Par1-/-* and *Par4-/-* mice and has conducted thrombin signaling assays to determine which thrombin receptors are present on endothelium (unpublished work of Hiroshi Kataoka). We can potentially derive endothelium from *Par1-/-Par4-/-* mice that is completely unresponsive to thrombin. Such cultures will allow us to perform a number of functional assays assays to understand the role of PAR1 in endothelial activation in the embryo. For example, we can ask whether *Par1-/-* endothelium can form tubules and tight junctions in culture assays. Additionally, cultured wildtype versus *Par1-/-* endothelium will allow us to analyze the expression levels and responsiveness to thrombin of a battery of candidate molecules by RT-PCR or protein detection to derive a better understanding of the signaling pathways through which PAR1 could be accomplishing its vascular effects. Another route the lab has been interested in exploring in an effort to understand what happens to *Par1-/-* endothelium at midgestation is that of performing pharmacological studies on cultured embryos. We could apply thrombin or activating peptide to cultured mouse embryos or yolk sacs and analyze the effects in real time using embryos with a transgenic endothelial-GFP reporter (such mice are currently available to the lab). Alternatively, we could utilize a simpler vertebrate model system with external development (i.e. zebrafish or frogs) to achieve a similar goal if the developmental effects of thrombin and PAR1 signaling are conserved across species.

In Chapter III we provided evidence that thrombin is a developmental ligand for PAR1 and that PAR4 appears to provide "back-up" thrombin signaling for PAR1 during development. In order to understand if the heightened lethality seen in *Par1-/-Par4-/-* embryos is due to loss of thrombin signaling on endothelium at the same time during

development, it will be important for us to conduct timed matings and to analyze the midgestational phenotype of *Par1-/-Par4-/-* versus *Par1-/-* embryos. The vascular expression of PAR4 at E9.5 (see Chapter 3, Fig. 11) provides evidence that the receptor is performing a redundant role with PAR1 at this time, but formal analysis is needed in case the increased lethality of doubly-deficient embryos is due to loss of thrombin signaling later in development. We have not thoroughly analyzed PAR4 expression patterns during late gestation to have an appreciation of other tissues and times at which PAR1 and PAR4 might play redundant roles. Embryonic dissections and genotyping will help us reject the possibility that late-gestational lethality accounts for the increased lethality of *Par1-/-Par4-/-* embryos. Provided that the doubly-deficient embryos are dying at E9.5, we will attempt to rescue the *Par1-/-Par4-/-* embryos with the TIE2p/e-PAR1 transgene that rescued the *Par1-/-* embryos (as described in Chapter II). Such rescue would provide more definitive proof that PAR4 and PAR1 play redundant roles in endothelial signaling at midgestation. We are also interested in trying to recapitulate the nearly 100% embryonic lethality reported for tissue factor-deficient embryos by two groups [*31,32*]. One group reported the influence of background strain on the penetrance of lethality; they achieved 100% lethality in a pure SV/129 background versus 86% lethality in a C57Bl/6-SV/129 background [*63*]. It will be important for us to determine whether we can achieve 100% lethality with our *Par1-/-Par4-/-* embryos (currently in a mixed C57Bl/6-SV/129 background) in order to rule out the possibility that still another effector of the coagulation cascade plays a role at midgestation. The existence of another effector is a real possibility since only one *FV-/-Par1-/-* embryo survived to E12.5 (see Chapter 3, Fig. 7). We currently possess inbred SV/129 and inbred C57Bl/6 *Par1-/-* and *Par4-/-*

mice that will allow us to explore the possibility of achieving a higher rate of embryonic lethality with doubly-deficient embryos.

The PARs are expressed after midgestation in unexpected places, as described in Chapter IV. The phenotypes of the knock-outs, however, have not instructed us in the roles of the receptors in late-gestation and in adulthood at these novel sites. We intend to use our *LacZ* knock-in embryos to determine whether we can unmask subtle phenotypes that can teach us more about protease signaling. For example, we might expect to detect disappearance of *LacZ*-positive cells or altered shape change or migration in homozygous versus heterozygous embryos that will instruct us in which cell types PAR function is important during development. Additionally, we intend to perform detailed histological analysis of the sites of expression, described at the whole-mount level in Chapter IV, to determine whether cellular phenotypes can be attributed to homozygous embryos. We are also interested in learning whether our knowledge of embryonic sites of PAR expression can instruct us in how to tease-out or enhance adult phenotypes in knock-out survivors. For example, models of intervertebral disc degeneration can be used to determine whether *Par1-/-* or *Par2-/-* discs are more prone to deterioration under stress *in vivo* [*86,87*]. Similarly, the embryonic patterns of PAR expression might direct our attention toward signaling pathways and molecules that could produce instructive new phenotypes when knocked-out in conjunction with the PARs. For example, WNT4 is expressed in the developing hair follicle, but, like PAR2, adult WNT4-deficient mice have no obvious defects in hair structure or production [*88*]. To determine whether the *Wnt* signaling pathway might converge with that of PAR2, *Wnt4-/-Par2-/-* mice could be bred and analyzed for novel hair defects.

Altogether, the work described in this thesis lays the groundwork for many exciting experiments that will elucidate the role of protease signaling in embryonic development. Presumably, the lessons we learn about the PARs in the embryo will enhance our knowledge of how and where the receptors function in the adult. Our lab has gained much knowledge about the role of PAR signaling in platelet activation over the past decade. The time is now ripe for expanding that knowledge to the roles of PARs in endothelium and other cell types, and the embryo provides a fascinating model for doing so.

Effect	Reference
Proliferation	[7]
Secretion of PDGF	[11]
Secretion of plasminogen activator-inhibitor	[89]
Production of prostacyclin	[90]
Production of thromboplastin	[91]
Expression of monocyte chemotactic protein-1	[92]
Increased tissue factor activity	[93]
Mobilization of P-selectin to the cell surface (accompanied by release of von Willebrand factor)	[52]
Secretion of extracellular matrix components (fibronectin, laminin, collagens IV and I)	[94]
Activation of progelatinase A	[42]
Enhanced mitogenic responses to:	
VEGF (plus upregulation of Flt-1)	[53]
FGF	[7]
Shape change (rounding) and retraction/ gap formation	[13,50,95,96]
Rearrangement of VE-cadherins and catenins	[51]
Permeability to proteins	[97]
Migration (in cooperation with VEGF, $\alpha v\beta 3$, and osteoponin)	[98]
Angiogenesis (CAM assay)	[99]

Table 3: Published effects induced by thrombin on endothelium in culture.

BIBLIOGRAPHY

1. Coughlin, S. R. Thrombin signalling and protease-activated receptors. *Nature* 407, 258-264 (2000).

2. Colman, R. W., Marder, V. J., Salzman, E. W. & Hirsh, J. in *Hemostasis and Thrombosis* (eds. Colman, R. W., Marder, V. J., Salzman, E. W. & Hirsh, J.) 3-18 (Lippincott, Philadelphia, 1994).

3. Davey, M. G. & Lüscher, E. F. Actions of thrombin and other coagulant and proteolytic enzymes on blood platelets. *Nature* 216, 857-858 (1967).

4. Berndt, M. & Phillips, D. in *Platelets in Biology and Pathology* (ed. Gordon, J. L.) 43-74 (Biomedical Press, Elsevier, North Holland, 1981).

5. Chen, L. B. & Buchanan, J. M. Mitogenic activity of blood components. I. Thrombin and prothrombin. *Proc. Natl. Acad. Sci. U.S.A.* 72, 131-135 (1975).

6. McNamara, C. A., Sarembock, I. J., Gimple, L. W., Fenton, J. W. d., Coughlin, S. R. & Owens, G. K. Thrombin stimulates proliferation of cultured rat aortic smooth muscle cells by a proteolytically activated receptor [see comments]. *J. Clin. Invest.* 91, 94-98 (1993).

7. Gospodarowicz, D., Brown, K. D., Birdwell, C. R. & Zetter, B. R. Control of proliferation of human vascular endothelial cells. Characterization of the response of human umbilical vein endothelial cells to fibroblast growth factor, epidermal growth factor, and thrombin. *J. Cell Biol.* 77, 774-788 (1978).

8. Naldini, A., Carney, D. H., Bocci, V., Klimpel, K. D., Asuncion, M., Soares, L. E. & Klimpel, G. R. Thrombin enhances T cell proliferative responses and cytokine production. *Cell. Immunol.* 147, 367-377 (1993).

9. Joseph, S. & MacDermot, J. The N-terminal thrombin receptor fragment SFLLRN, but not catalytically inactive thrombin-derived agonists, activate U937 human monocytic cells: evidence for receptor hydrolysis in thrombin-dependent signalling. *Biochem. J.* 290, 571-577 (1993).

10. Bizios, R., Lai, L., Fenton, J. W. d. & Malik, A. B. Thrombin-induced chemotaxis and aggregation of neutrophils. *J. Cell. Physiol.* 128, 485-490 (1986).

11. Daniel, T. O., Gibbs, V. C., Milfay, D. F., Garovoy, M. R. & Williams, L. T. Thrombin stimulates c-sis gene expression in microvascular endothelial cells. *J. Biol. Chem.* 261, 9579-9582 (1986).

12. Kranzhöfer, R., Clinton, S. K., Ishii, K., Coughlin, S. R., Fenton, J. W., 2nd & Libby, P. Thrombin potently stimulates cytokine production in human vascular smooth muscle cells but not in mononuclear phagocytes. *Circ. Res.* 79, 286-294 (1996).

13. Lum, H. & Malik, A. B. Regulation of vascular endothelial barrier function. *Am. J. Physiol.* 267, L223-241 (1994).

14. Vu, T. K., Hung, D. T., Wheaton, V. I. & Coughlin, S. R. Molecular cloning of a functional thrombin receptor reveals a novel proteolytic mechanism of receptor activation. *Cell* 64, 1057-1068 (1991).

15. Ishihara, H., Connolly, A. J., Zeng, D., Kahn, M. L., Zheng, Y. W., Timmons, C., Tram, T. & Coughlin, S. R. Protease-activated receptor 3 is a second thrombin receptor in humans. *Nature* 386, 502-506 (1997).

16. Kahn, M. L., Zheng, Y. W., Huang, W., Bigornia, V., Zeng, D., Moff, S., Farese, R. V., Jr., Tam, C. & Coughlin, S. R. A dual thrombin receptor system for platelet activation. *Nature* 394, 690-694 (1998).

17. Nystedt, S., Emilsson, K., Wahlestedt, C. & Sundelin, J. Molecular cloning of a potential proteinase activated receptor [see comments]. *Proc. Natl. Acad. Sci. U.S.A.* 91, 9208-9212 (1994).

18. Molino, M., Barnathan, E. S., Numerof, R., Clark, J., Dreyer, M., Cumashi, A., Hoxie, J. A., Schechter, N., Woolkalis, M. & Brass, L. F. Interactions of mast cell tryptase with thrombin receptors and PAR-2. *J. Biol. Chem.* 272, 4043-4049 (1997).

19. Camerer, E., Huang, W. & Coughlin, S. R. Tissue factor- and factor X-dependent activation of protease-activated receptor 2 by factor VIIa. *Proc. Natl. Acad. Sci. U.S.A.* 97, 5255-5260 (2000).

20. Connolly, A. J., Ishihara, H., Kahn, M. L., Farese, R. V., Jr. & Coughlin, S. R. Role of the thrombin receptor in development and evidence for a second receptor. *Nature* 381, 516-519 (1996).

21. Trejo, J., Connolly, A. J. & Coughlin, S. R. The cloned thrombin receptor is necessary and sufficient for activation of mitogen-activated protein kinase and mitogenesis in mouse lung fibroblasts. Loss of responses in fibroblasts from receptor knockout mice. *J. Biol. Chem.* 271, 21536-21541 (1996).

22. Connolly, A. J., Suh, D. Y., Hunt, T. K. & Coughlin, S. R. Mice lacking the thrombin receptor, PAR1, have normal skin wound healing. *Am. J. Path.* 151, 1199-1204 (1997).

23. Nakanishi-Matsui, M., Zheng, Y. W., Sulciner, D. J., Weiss, E. J., Ludeman, M. J. & Coughlin, S. R. PAR3 is a cofactor for PAR4 activation by thrombin. *Nature* 404, 609-613 (2000).

24. Sambrano, G. R., Zheng, Y. W., Weiss, E. J., Huang, W. & Coughlin, S. R. , manuscript in preparation.

25. Darrow, A. L., Fung, L. W., Ye, R. D., Santulli, R. J., Cheung, W. M., Derian, C. K., Burns, C. L., Damiano, B. P., Zhou, L., Keenan, C. M., Peterson, P. A. & Andrade, G. P. Biological consequences of thrombin receptor deficiency in mice. *Thromb. Haemost.* 76, 860-866 (1996).

26. Esmon, C. T., Fukudome, K., Mather, T., Bode, W., Regan, L. M., Stearns-Kurosawa, D. J. & Kurosawa, S. Inflammation, sepsis, and coagulation. *Haematologica* 84, 254-259 (1999).

27. Soifer, S. J., Peters, K. G., O'Keefe, J. & Coughlin, S. R. Disparate temporal expression of the prothrombin and thrombin receptor genes during mouse development. *Am. J. Path.* 144, 60-69 (1994).

28. Drake, T. A., Morrissey, J. H. & Edgington, T. S. Selective cellular expression of tissue factor in human tissues. Implications for disorders of hemostasis and thrombosis. *Am. J. Path.* 134, 1087-1097 (1989).

29. Bevilacqua, M. P. & Gimbrone, M. A., Jr. Inducible endothelial functions in inflammation and coagulation. *Semin. Thromb. Hemost.* 13, 425-433 (1987).

30. Degen, J. L. Hemostatic factors and inflammatory disease. *Thromb. Haemost.* 82, 858-864 (1999).

31. Bugge, T. H., Xiao, Q., Kombrinck, K. W., Flick, M. J., Holmbäck, K., Danton, M. J., Colbert, M. C., Witte, D. P., Fujikawa, K., Davie, E. W. & Degen, J. L. Fatal embryonic bleeding events in mice lacking tissue factor, the cell-associated initiator of blood coagulation. *Proc. Natl. Acad. Sci. U.S.A.* 93, 6258-6263 (1996).

32. Carmeliet, P., Mackman, N., Moons, L., Luther, T., Gressens, P., Van, V. I., Demunck, H., Kasper, M., Breier, G., Evrard, P., Muller, M., Risau, W., Edgington, T. & Collen, D. Role of tissue factor in embryonic blood vessel development. *Nature* 383, 73-75 (1996).

33. Toomey, J. R., Kratzer, K. E., Lasky, N. M., Stanton, J. J. & Broze, G. J., Jr. Targeted disruption of the murine tissue factor gene results in embryonic lethality. *Blood* 88, 1583-1587 (1996).

34. Dewerchin, M., Liang, Z., Moons, L., Carmeliet, P., Castellino, F. J., Collen, D. & Rosen, E. D. Blood coagulation factor X deficiency causes partial embryonic lethality and fatal neonatal bleeding in mice. *Thromb. Haemost.* 83, 185-190 (2000).

35. Cui, J., O'Shea, K. S., Purkayastha, A., Saunders, T. L. & Ginsburg, D. Fatal haemorrhage and incomplete block to embryogenesis in mice lacking coagulation factor V. *Nature* 384, 66-68 (1996).

36. Sun, W. Y., Witte, D. P., Degen, J. L., Colbert, M. C., Burkart, M. C., Holmbäck, K., Xiao, Q., Bugge, T. H. & Degen, S. J. Prothrombin deficiency results in embryonic and neonatal lethality in mice. *Proc. Natl. Acad. Sci. U.S.A.* 95, 7597-7602 (1998).

37. Xue, J., Wu, Q., Westfield, L. A., Tuley, E. A., Lu, D., Zhang, Q., Shim, K., Zheng, X. & Sadler, J. E. Incomplete embryonic lethality and fatal neonatal hemorrhage

caused by prothrombin deficiency in mice. *Proc. Natl. Acad. Sci. U.S.A.* 95, 7603-7607 (1998).

38. Shivdasani, R. A., Rosenblatt, M. F., Zucker, F. D., Jackson, C. W., Hunt, P., Saris, C. J. & Orkin, S. H. Transcription factor NF-E2 is required for platelet formation independent of the actions of thrombopoietin/MGDF in megakaryocyte development. *Cell* 81, 695-704 (1995).

39. Rosen, E. D., Chan, J. C., Idusogie, E., Clotman, F., Vlasuk, G., Luther, T., Jalbert, L. R., Albrecht, S., Zhong, L., Lissens, A., Schoonjans, L., Moons, L., Collen, D., Castellino, F. J. & Carmeliet, P. Mice lacking factor VII develop normally but suffer fatal perinatal bleeding. *Nature* 390, 290-294 (1997).

40. Auerbach, R., Huang, H, Lisheng, L. Hematopoietic stem cells in the mouse embryonic yolk sac. *Stem Cells* 14, 269-280 (1996).

41. Schlaeger, T. M., Bartunkova, S., Lawitts, J. A., Teichmann, G., Risau, W., Deutsch, U. & Sato, T. N. Uniform vascular-endothelial-cell-specific gene expression in both embryonic and adult transgenic mice. *Proc. Natl. Acad. Sci. U.S.A.* 94, 3058-3063 (1997).

42. Hattori, R., Hamilton, K. K., Fugate, R. D., McEver, R. P. & Sims, P. J. Stimulated secretion of endothelial von Willebrand factor is accompanied by rapid redistribution to the cell surface of the intracellular granule membrane protein GMP-140. *J. Biol. Chem.* 264, 7768-7771 (1989).

43. Palabrica, T., Lobb, R., Furie, B. C., Aronovitz, M., Benjamin, C., Hsu, Y. M., Sajer, S. A. & Furie, B. Leukocyte accumulation promoting fibrin deposition is mediated in vivo by P-selectin on adherent platelets. *Nature* 359, 848-851 (1992).

44. Subramaniam, M., Frenette, P. S., Saffaripour, S., Johnson, R. C., Hynes, R. O. & Wagner, D. D. Defects in hemostasis in P-selectin-deficient mice. *Blood* 87, 1238-1242 (1996).

45. Offermanns, S., Toombs, C. F., Hu, Y. H. & Simon, M. I. Defective platelet activation in G alpha(q)-deficient mice. *Nature* 389, 183-186 (1997).

46. Suh, T. T., Holmback, K., Jensen, N. J., Daugherty, C. C., Small, K., Simon, D. I., Potter, S. & Degen, J. L. Resolution of spontaneous bleeding events but failure of pregnancy in fibrinogen-deficient mice. *Genes Dev.* 9, 2020-2033 (1995).

47. Ogawa, S., Gerlach, H., Esposito, C., Pasagian-Macaulay, A., Brett, J. & Stern, D. Hypoxia modulates the barrier and coagulant function of cultured bovine endothelium. Increased monolayer permeability and induction of procoagulant properties. *J. Clin. Invest.* 85, 1090-1098 (1990).

48. Gertler, J. P., Weibe, D. A., Ocasio, V. H. & Abbott, W. M. Hypoxia induces procoagulant activity in cultured human venous endothelium. *J. Vasc. Surg.* 13, 428-433 (1991).

49. Lawson, C. A., Yan, S. D., Yan, S. F., Liao, H., Zhou, Y. S., Sobel, J., Kisiel, W., Stern, D. M. & Pinsky, D. J. Monocytes and tissue factor promote thrombosis in a murine model of oxygen deprivation. *J. Clin. Invest.* 99, 1729-1738 (1997).

50. Vouret-Craviari, V., Boquet, P., Pouysségur, J. & Van Obberghen-Schilling, E. Regulation of the actin cytoskeleton by thrombin in human endothelial cells: role of Rho proteins in endothelial barrier function. *Mol. Biol. Cell* 9, 2639-2653 (1998).

51. Rabiet, M. J., Plantier, J. L., Rival, Y., Genoux, Y., Lampugnani, M. G. & Dejana, E. Thrombin-induced increase in endothelial permeability is associated with

changes in cell-to-cell junction organization. *Arterioscler. Thromb. Vasc. Biol.* 16, 488-496 (1996).

52. Papadimitriou, E., Manolopoulos, V. G., Hayman, G. T., Maragoudakis, M. E., Unsworth, B. R., Fenton, J. W., 2nd & Lelkes, P. I. Thrombin modulates vectorial secretion of extracellular matrix proteins in cultured endothelial cells. *Am. J. Physiol.* 272, C1112-1122 (1997).

53. Tsopanoglou, N. E. & Maragoudakis, M. E. On the mechanism of thrombin-induced angiogenesis. Potentiation of vascular endothelial growth factor activity on endothelial cells by up-regulation of its receptors. *J. Biol. Chem.* 274, 23969-23976 (1999).

54. Srinivasan, Y., Lovicu, F. J. & Overbeek, P. A. Lens-specific expression of transforming growth factor beta1 in transgenic mice causes anterior subcapsular cataracts. *J. Clin. Invest.* 101, 625-634 (1998).

55. Schlaeger, T. M., Qin, Y., Fujiwara, Y., Magram, J. & Sato, T. N. Vascular endothelial cell lineage-specific promoter in transgenic mice. *Development* 121, 1089-1098 (1995).

56. Roberts, H. R. & Lefkowitz, J. B. in *Hemostasis and Thrombosis* (eds. Colman, R. W., Hirsh, J., Marder, V. J. & Salzman, E. W.) 200-218 (J.B. Lippincott Company, Philadelphia, 1994).

57. Seeler, R. A. Parahemophilia. Factor V deficiency. *Br. J. Haematol.* 56, 119-125 (1972).

58. Tracy, P. B. & Mann, K. G. Abnormal formation of the prothrombinase complex: factor V deficiency and related disorders. *Hum. Pathol.* 18, 162-169 (1987).

59. Guasch, J. F., Cannegieter, S., Reitsma, P. H., van't Veer-Korthof, E. T. & Bertina, R. M. Severe coagulation factor V deficiency caused by a 4 bp deletion in the factor V gene. *Br. J. Haematol.* 101, 32-39 (1998).

60. Cooper, D. N., Millar, D. S., Wacey, A., Pemberton, S. & Tuddenham, E. G. Inherited factor X deficiency: molecular genetics and pathophysiology. *Thromb. Haemost.* 78, 161-172 (1997).

61. Kahn, M. L., Nakanishi-Matsui, M., Shapiro, M. J., Ishihara, H. & Coughlin, S. R. Protease-activated receptors 1 and 4 mediate activation of human platelets by thrombin. *J. Clin. Invest.* 103, 879-887 (1999).

62. Shapiro, M. J., Weiss, E. J., Faruqi, T. R. & Coughlin, S. R. Protease-activated receptors 1 and 4 are shut off with distinct kinetics after activation by thrombin. *J. Biol. Chem.* 275, 25216-25221 (2000).

63. Toomey, J. R., Kratzer, K. E., Lasky, N. M. & Broze, G. J., Jr. Effect of tissue factor deficiency on mouse and tumor development. *Proc. Natl. Acad. Sci. U.S.A.* 94, 6922-6926 (1997).

64. Santulli, R. J., Derian, C. K., Darrow, A. L., Tomko, K. A., Eckardt, A. J., Seiberg, M., Scarborough, R. M. & Andrade-Gordon, P. Evidence for the presence of a protease-activated receptor distinct from the thrombin receptor in human keratinocytes. *Proc. Natl. Acad. Sci. U.S.A.* 92, 9151-9155 (1995).

65. Faruqi, T. R., Weiss, E. J., Shapiro, M. J., Hung, W. & Coughlin, S. R. Structure-function analysis of protease-activated receptor-4 tethered tigand peptides: Determinants of specificity and utility in assays of receptor function. *J. Biol. Chem.* 275, 19728-19734 (2000).

66. Xu, W. F., Andersen, H., Whitmore, T. E., Presnell, S. R., Yee, D. P., Ching, A., Gilbert, T., Davie, E. W. & Foster, D. C. Cloning and characterization of human protease-activated receptor 4. *Proc. Natl. Acad. Sci. U.S.A.* 95, 6642-6646 (1998).

67. Hogan, B., Beddington, R., Constantini, F. & Lacy, E. *Manipulating the mouse embryo* (Cold Spring Harbor Laboratory Press, 1994).

68. Sambrook, J. & Russell, D. W. *Molecular Cloning: A Laboratory Manual* (Cold Spring Harbor Laboratory Press, Cold Spring Harbor, NY, 2001).

69. Lewandoski, M., Meyers, E. N. & Martin, G. R. Analysis of Fgf8 gene function in vertebrate development. *Cold Spring Harb. Symp. Quant. Biol.* 62, 159-168 (1997).

70. Olson, E. N., Arnold, H. H., Rigby, P. W. & Wold, B. J. Know your neighbors: three phenotypes in null mutants of the myogenic bHLH gene MRF4. *Cell* 85, 1-4 (1996).

71. Faust, N., Varas, F., Kelly, L. M., Heck, S. & Graf, T. Insertion of enhanced green fluorescent protein into the lysozyme gene creates mice with green fluorescent granulocytes and macrophages. *Blood* 96, 719-726 (2000).

72. Kaufman, M. H. *The Atlas of Mouse Development* (Academic Press, Inc., San Diego, California, 1992).

73. Rufai, A., Benjamin, M. & Ralphs, J. R. The development of fibrocartilage in the rat intervertebral disc. *Anat. Embryol.* 192, 53-62 (1995).

74. Kahn, M. L., Hammes, S. R., Botka, C. & Coughlin, S. R. Gene and locus structure and chromosomal localization of the protease-activated receptor gene family. *J. Biol. Chem.* 273, 23290-23296 (1998).

75. Gilbert, S. F. *Developmental Biology, Fourth Edition* (Sinauer Associates, Inc., Sunderland, Massachusetts, 1994).

76. Mortensen, R. in *Current Protocols in Molecular Biology* (ed. Ausubel, F. M. e. a.) 9.16.11 (J. Wiley & Sons, Inc., New York, 1993).

77. Sauer, B. in *Guide to Techniques in Mouse Development* (eds. Wassarman, P. M. & DePamphilis, M. L.) 890-900 (Academic Press, Inc., San Diego, 1993).

78. Meiner, V. L., Cases, S., Myers, H. M., Sande, E. R., Bellosta, S., Schambelan, M., Pitas, R. E., McGuire, J., Herz, J. & Farese, R. V., Jr. Disruption of the acyl-CoA:cholesterol acyltransferase gene in mice: evidence suggesting multiple cholesterol esterification enzymes in mammals. *Proc. Natl. Acad. Sci. U.S.A.* 93, 14041-14046 (1996).

79. Carmeliet, P., Ferreira, V., Breier, G., Pollefeyt, S., Kieckens, L., Gertsenstein, M., Fahrig, M., Vandenhoeck, A., Harpal, K., Eberhardt, C., Declercq, C., Pawling, J., Moons, L., Collen, D., Risau, W. & Nagy, A. Abnormal blood vessel development and lethality in embryos lacking a single VEGF allele. *Nature* 380, 435-439 (1996).

80. Ferrara, N., Carver-Moore, K., Chen, H., Dowd, M., Lu, L., O'Shea, K. S., Powell-Braxton, L., Hillan, K. J. & Moore, M. W. Heterozygous embryonic lethality induced by targeted inactivation of the VEGF gene. *Nature* 380, 439-442 (1996).

81. Fong, G. H., Rossant, J., Gertsenstein, M. & Breitman, M. L. Role of the Flt-1 receptor tyrosine kinase in regulating the assembly of vascular endothelium. *Nature* 376, 66-70 (1995).

82. Shalaby, F., Rossant, J., Yamaguchi, T. P., Gertsenstein, M., Wu, X. F., Breitman, M. L. & Schuh, A. C. Failure of blood-island formation and vasculogenesis in Flk-1-deficient mice. *Nature* 376, 62-66 (1995).

83. Dumont, D. J., Jussila, L., Taipale, J., Lymboussaki, A., Mustonen, T., Pajusola, K., Breitman, M. & Alitalo, K. Cardiovascular failure in mouse embryos deficient in VEGF receptor-3. *Science* 282, 946-949 (1998).

84. Suri, C., Jones, P. F., Patan, S., Bartunkova, S., Maisonpierre, P. C., Davis, S., Sato, T. N. & Yancopoulos, G. D. Requisite role of angiopoietin-1, a ligand for the TIE2 receptor, during embryonic angiogenesis [see comments]. *Cell* 87, 1171-1180 (1996).

85. Sato, T. N., Tozawa, Y., Deutsch, U., Wolburg-Buchholz, K., Fujiwara, Y., Gendron-Maguire, M., Gridley, T., Wolburg, H., Risau, W. & Qin, Y. Distinct roles of the receptor tyrosine kinases Tie-1 and Tie-2 in blood vessel formation. *Nature* 376, 70-74 (1995).

86. Lotz, J. C. & Chin, J. R. Intervertebral disc cell death is dependent on the magnitude and duration of spinal loading. *Spine* 25, 1477-1483 (2000).

87. Lotz, J. C., Colliou, O. K., Chin, J. R., Duncan, N. A. & Liebenberg, E. Compression-induced degeneration of the intervertebral disc: an in vivo mouse model and finite-element study. *Spine* 23, 2493-2506 (1998).

88. Kishimoto, J., Burgeson, R. E. & Morgan, B. A. Wnt signaling maintains the hair-inducing activity of the dermal papilla. *Genes Dev.* 14, 1181-1185 (2000).

89. Gelehrter, T. D. & Sznycer-Laszuk, R. Thrombin induction of plasminogen activator-inhibitor in cultured human endothelial cells. *J. Clin. Invest.* 77, 165-169 (1986).

90. Weksler, B. B., Ley, C. W. & Jaffe, E. A. Stimulation of endothelial cell prostacyclin production by thrombin, trypsin, and the ionophore A 23187. *J. Clin. Invest.* 62, 923-930 (1978).

91. Galdal, K. S., Lyberg, T., Evensen, S. A., Nilsen, E. & Prydz, H. Thrombin induces thromboplastin synthesis in cultured vascular endothelial cells. *Thromb. Haemost.* 54, 373-376 (1985).

92. Colotta, F., Sciacca, F. L., Sironi, M., Luini, W., Rabiet, M. J. & Mantovani, A. Expression of monocyte chemotactic protein-1 by monocytes and endothelial cells exposed to thrombin. *Am. J. Pathol.* 144, 975-985 (1994).

93. Bartha, K., Brisson, C., Archipoff, G., de la Salle, C., Lanza, F., Cazenave, J. P. & Beretz, A. Thrombin regulates tissue factor and thrombomodulin mRNA levels and activities in human saphenous vein endothelial cells by distinct mechanisms. *J. Biol. Chem.* 268, 421-429 (1993).

94. Zucker, S., Conner, C., DiMassmo, B. I., Ende, H., Drews, M., Seiki, M. & Bahou, W. F. Thrombin induces the activation of progelatinase A in vascular endothelial cells. Physiologic regulation of angiogenesis. *J. Biol. Chem.* 270, 23730-23738 (1995).

95. Galdal, K. S., Evensen, S. A. & Brosstad, F. Effects of thrombin on the integrity of monolayers of cultured human endothelial cells. *Thromb. Res.* 27, 575-584 (1982).

96. Laposata, M., Dovnarsky, D. K. & Shin, H. S. Thrombin-induced gap formation in confluent endothelial cell monolayers in vitro. *Blood* 62, 549-556 (1983).

97. Garcia, J. G., Siflinger-Birnboim, A., Bizios, R., Del Vecchio, P. J., Fenton, J. W. d. & Malik, A. B. Thrombin-induced increase in albumin permeability across the endothelium. *J. Cell. Physiol.* 128, 96-104 (1986).

98. Senger, D. R., Ledbetter, S. R., Claffey, K. P., Papadopoulos, S. A., Peruzzi, C. A. & Detmar, M. Stimulation of endothelial cell migration by vascular permeability factor/vascular endothelial growth factor through cooperative mechanisms involving the alphavbeta3 integrin, osteopontin, and thrombin. *Am. J. Pathol.* 149, 293-305 (1996).

99. Tsopanoglou, N. E., Pipili, S. E. & Maragoudakis, M. E. Thrombin promotes angiogenesis by a mechanism independent of fibrin formation. *Am. J. Physiol.*, C1302-1307 (1993).